

## Statistical properties of polarons in a magnetic field. II. Numerical results and discussion on the phase transition

F. M. Peeters

*Departement Natuurkunde, Universitaire Instelling Antwerpen (UIA), Universiteitsplein 1, B-2610 Wilrijk, Belgium*

J. T. Devreese

*Departement Natuurkunde, Universitaire Instelling Antwerpen (UIA) and Rijksuniversitair Centrum Antwerpen (RUCA), Universiteitsplein 1, B-2610 Wilrijk, Belgium and Technische Hogeschool Eindhoven, Eindhoven, The Netherlands*  
(Received 3 November 1981; revised manuscript received 12 March 1982)

A detailed numerical analysis is made of the analytic results presented in paper I. Numerical results are presented for the mass of the Feynman polaron, parallel ( $M_{\parallel}$ ) and perpendicular ( $M_{\perp}$ ) to the magnetic field, and for the following thermodynamic quantities: the magnetization, the susceptibility, the internal energy, the entropy, and the specific heat. Those quantities are studied for different values of the electron-phonon coupling ( $\alpha$ ), temperature ( $T$ ), and magnetic field strength ( $\mathcal{H}$ ). We found that an ideal gas of polarons undergoes a phase transition. In the physical parameter space ( $1/\alpha, 1/\mathcal{H}, T$ ) the points of first-order phase transition define a two-dimensional surface which is circumscribed by a line of second-order phase transitions. At the transition point the polaron transforms in the direction perpendicular to the magnetic field, and with increasing magnetic field strength, from a polaron state ( $M_{\parallel} \approx M_{\perp}$ ) to an almost free Landau state ( $M_{\parallel} \gg M_{\perp} \sim 1$ ). This transition can be viewed as a magnetic-field-induced two-dimensional stripping of the polaron. The experimental consequences of this phase transition on the thermodynamic quantities and the magneto-optical absorption spectrum are discussed.

### I. INTRODUCTION

In the preceding paper<sup>1</sup> (hereafter referred to as I) we derived an approximate expression for the polaron free energy ( $F$ ), which is valid for all values of the magnetic field ( $\mathcal{H}$ ), the temperature ( $T$ ), and the electron-phonon coupling strength ( $\alpha$ ). This expression was obtained by extending Feynman's polaron theory<sup>2</sup> to include (1) an external magnetic field and (2) an anisotropic effective electron-phonon interaction. According to Feynman's conjecture the free energy as derived in I is an upper bound to the exact free energy. The explicit form of the free energy depends on four variational parameters. The variational calculation has to be performed numerically except for certain limiting cases where analytic results could be obtained (see Sec. V of paper I). In the present paper (hereafter referred to as II) emphasis is placed on the numerical study of the analytical results presented in paper I. After the numerical variational calculation we obtain results for the free energy that depend on three physical parameters:  $\alpha$ ,

$T$ , and  $\omega_c = e\mathcal{H}/mc$  ( $e$  is the electron charge,  $m$  the electron band mass, and  $c$  the velocity of light). From the free energy we calculate the magnetization  $\mathcal{M} = -\partial F/\partial \mathcal{H}$ , the susceptibility  $\chi = -\partial^2 F/\partial \mathcal{H}^2$ , the entropy  $S = -\partial F/\partial T$ , the internal energy  $E = F + TS$ , and the specific heat  $C = -T\partial^2 F/\partial T^2$ . Figures of these quantities are presented for different values of  $\alpha$ ,  $T$ , and  $\omega_c$ .

To the best of our knowledge, the present paper constitutes the first detailed study of the different thermodynamic functions of an ideal polaron gas for arbitrary  $\alpha$ ,  $T$ , and  $\omega_c$ . Most of the previous studies on the thermodynamic properties of the polaron system are confined to the calculation of the ground-state energy. There exist a few calculations of the polaron susceptibility in the small magnetic field limit. Namely, Hellwarth and Platzman<sup>3</sup> calculated the polaron diamagnetic susceptibility for small magnetic fields and low temperature by using Feynman's path-integral formalism and by using the same ("symmetrical") trial action as in Feynman's polaron theory.<sup>2</sup> Recently, Saitoh<sup>4,5</sup> revisited this calculation and used a more general tri-

al action to calculate  $\chi$  for small magnetic fields and arbitrary temperature. The calculations in Refs. 3 and 4 are intended to be valid for arbitrary  $\alpha$ . In Ref. 5 Saitoh extended his calculation to arbitrary magnetic field strength. Only analytic results were presented; no numerical analysis was made in Ref. 5.

The numerical study of the problem reveals interesting phenomena. Namely, for certain values of  $\alpha$ ,  $T$ , and  $\omega_c$  the ideal gas of polarons undergoes a phase transition. At the phase-transition point the polaron transforms in the direction perpendicular to the magnetic field, and with increasing magnetic field strength, from a *polaronlike state* with  $M_{\parallel} \approx M_{\perp}$  to an *almost-free-electron state* with  $M_{\parallel} \gg M_{\perp} \sim m$  [here  $M_{\parallel} = (v_{\parallel}/w_{\parallel})^2$  and  $M_{\perp} = (v_{\perp}/w_{\perp})^2$  are the masses of the Feynman polaron, respectively, parallel and perpendicular to the magnetic field]. Thus at the phase-transition point the effective electron-phonon interaction in the direction perpendicular to the magnetic field changes abruptly. Parallel to the magnetic field no large changes in the effective electron-phonon interaction (and thus in  $M_{\parallel}$ ) are found at the transition point. As a consequence of this phase transition the thermodynamic functions  $\mathcal{M}$ ,  $\chi$ ,  $E$ ,  $S$ , and  $C$  exhibit a discontinuity at the transition point. Those discontinuities, found in the derivatives of the free energy, are a property of our model calculation and may or may not exist in the exact result. However, the exact result, of course, is not known.

Previously, we reported<sup>6</sup> briefly on the existence of the phase transition of the ideal polaron gas in the special case of zero temperature. For  $T=0$  the phase diagram consists of a curve of first-order phase transitions that starts in the "critical" point ( $\alpha = 4.20 \pm 0.01, \omega_c/\omega_0 = 2.24 \pm 0.01$ ) where a second-order phase transition occurs. Increasing  $\alpha$  ( $\alpha > 4.2$ ) increases the critical magnetic field at which the transition occurs. For  $\alpha \leq 4.2$  no phase transition is found at zero temperature. In this paper we extend the previous results to arbitrary temperature and found that the line of first-order phase transitions at zero temperature is extended to a two-dimensional surface in the three-dimensional space  $\alpha, T, \omega_c$ . The critical point at zero temperature becomes a critical curve which circumscribes the plane of first-order phase transitions.

In the past several investigators<sup>7-12</sup> have claimed,<sup>13</sup> or suggested, that the polaron would exhibit a transition at a specific  $\alpha$  value for  $T=0$  and  $\omega_c=0$ . The polaron would transform from a free to a self-trapped state. We have reviewed the

status of this problem in Ref. 14, where we showed numerically that the Feynman polaron theory gives a smooth transition ( $\partial E/\partial\alpha$  and  $\partial^2 E/\partial\alpha^2$  are continuous) between the weak and the strong electron-phonon coupling region, while the approximation of Refs. 7-12 lead to a discontinuous behavior of  $\partial E/\partial\alpha$  and/or (depending on the approximation considered)  $\partial^2 E/\partial\alpha^2$  as a function of  $\alpha$ . Although the Feynman polaron theory provides lower values for the polaron ground-state energy than the approaches of Refs. 7 and 9-12, the above reasoning does not prove that the exact polaron ground-state energy would have continuous derivatives.

If the polaron also interacts with acoustical phonons, Toyozawa<sup>15</sup> showed that the above-mentioned localization-type of phase transition is possible. Contrary to the phase transition predicted by Toyozawa (involving acoustical phonons) the phase transition reported here is induced by the application of a magnetic field. Of course it is conceivable that other external fields, e.g., an electric field, might also induce a change of polaron state. The phase transition studied in the present work is tentatively ascribed to the "stripping" of a polaron. Namely, if the velocity of the polaron becomes sufficiently large, the polarization cloud surrounding the electron will no longer be able to follow the electron and will be stripped off. The polaron then transforms to a free electron. In the problem under study the stripping of the polaron occurs only in two dimensions, namely in the direction perpendicular to the magnetic field.

The present paper is organized as follows. The first two sections deal with the zero-temperature case. In Sec. II the behavior of the polaron masses  $M_{\perp}$  and  $M_{\parallel}$ , the magnetization and the susceptibility, is studied as a function of the magnetic field for small and intermediate values of the electron-phonon coupling strength. A detailed numerical comparison between different theories is presented. Sec. III deals with the phase transition of the ideal polaron gas occurring if  $\alpha \geq 4.2$ . Thermodynamic quantities are studied in the vicinity of the critical point. A phase diagram is plotted and an order parameter is defined. In Sec. IV the magnetic field is taken equal to zero (thus  $M_{\perp} = M_{\parallel}$ ) and the polaron mass, the internal energy, the entropy, and the specific heat are studied as a function of the temperature for different values of  $\alpha$ . In the specific heat a peak is found to occur at  $T/T_D = 0.20 \pm 0.01$  (with  $T_D = \hbar\omega_0/k_B$ ;  $k_B$  is the Boltzmann constant) whose position turns out to

be  $\alpha$  independent. The combined influence of temperature and a magnetic field on the phase-transition behavior of the polaron is studied in Sec. V, first as a function of the magnetic field and subsequently as a function of temperature. It is found that the critical point ( $\alpha=4.2, \omega_c/\omega_0=2.24$ ) shifts to smaller  $\alpha$  and smaller  $\omega_c$  values if temperature increases. A plot of the three-dimensional phase diagram is presented. In Sec. VI concluding remarks are presented. We comment on the difference between the present approach and a mean-field-type approach. The experimental implications of the present theoretical results are critically discussed. The units used in the present paper are such that  $\hbar=m=\omega_0=1$ .

## II. SMALL- AND INTERMEDIATE-COUPLING BEHAVIOR OF THE IDEAL POLARON GAS AS A FUNCTION OF THE MAGNETIC FIELD (ZERO TEMPERATURE)

### A. Polaron ground-state energy, the magnetization, the susceptibility, and the mass of the Feynman polaron

In Fig. 1 the ground-state energy (solid curve) of one polaron is plotted as a function of the magnetic field for  $\alpha=1$ . For comparison we plotted the ground-state energy of a free electron (dotted curve) in a magnetic field. The influence of the electron-phonon interaction on the electron can be understood as follows. First, the electron-phonon interaction results in a binding energy which, at  $\omega_c=0$  and for small  $\alpha$  is proportional to  $-\alpha$ . This shifts the dotted curve to the dashed curve in Fig. 1. Second, the quantum states to be studied in a magnetic field are those of a quasiparticle—the polaron—with mass  $m^*$ . This results in the dashed-dotted curve in Fig. 1, which corresponds to the effective-mass approximation to the polaron ground-state energy. Larsen<sup>16</sup> has shown that the effective-mass approximation is only valid for small magnetic fields. Figure 1 confirms Larsen's statement. With increasing magnetic field the effective-mass approximation breaks down because the polaron can no longer be considered as a rigid particle with a well-defined mass.

The mass of the Feynman polaron perpendicular,  $M_{\perp}=(v_{\perp}/w_{\perp})^2$ , and parallel,  $M_{\parallel}=(v_{\parallel}/w_{\parallel})^2$ , to the magnetic field is shown in Fig. 2 for different values of the electron-phonon coupling constant  $\alpha$ , namely  $\alpha=1, 2$ , and 3. As discussed in

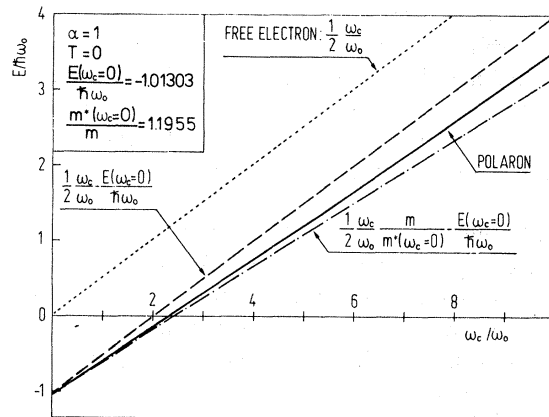


FIG. 1. Polaron ground-state energy (solid curve) as function of the magnetic field for  $\alpha=1$  and at zero temperature. The lowest unperturbed Landau energy level (dotted curve) and the same shifted with the polaron binding energy at zero magnetic field (dashed curve) are drawn for comparison. For small magnetic field values the polaron energy follows closely the lowest Landau level of a particle with mass  $m^*$  ( $\omega_c=0$ ) (which is the polaron mass at zero magnetic field) shifted with the polaron binding energy at zero magnetic field (dashed-dotted curve).

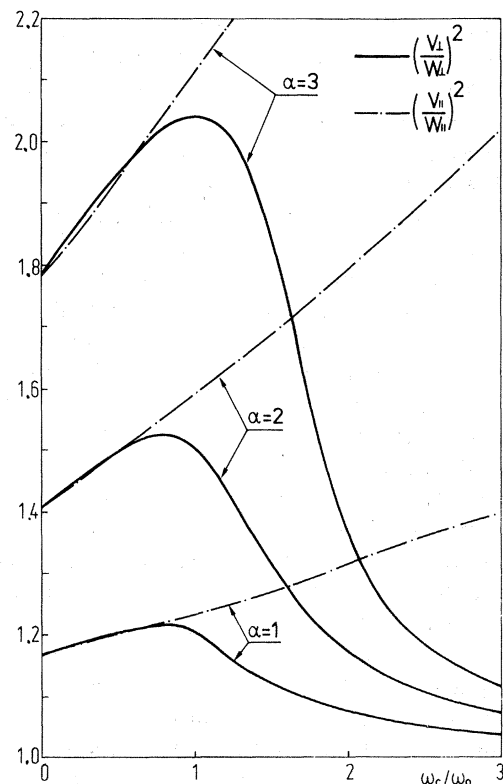


FIG. 2. Masses of the Feynman polaron perpendicular,  $M_{\perp}=(v_{\perp}/w_{\perp})^2$ , and parallel,  $M_{\parallel}=(v_{\parallel}/w_{\parallel})^2$ , to the magnetic field for  $\alpha=1, 2, 3$  and at zero temperature.

paper I, the masses  $M_{\perp}$  and  $M_{\parallel}$  are a measure of the effective interaction between the electron and the phonon field. To understand Fig. 2 it should be realized that two interaction mechanisms, which impose a different symmetry on the electron wave function, are involved in the problem. The interaction of the electron with the magnetic field imposes axial symmetry, while the electron-phonon interaction has spherical symmetry.

In the absence of a magnetic field the electron wave function is spherical symmetrical and thus  $M_{\perp} = M_{\parallel}$ . Applying a magnetic field results in a decrease of the radius<sup>17</sup> of the electron wave function perpendicular to the magnetic field. Consequently, as a function of  $\omega_c$  the electron tends to localize in the direction perpendicular to the magnetic field; this results in an increase of the effective electron-phonon interaction and therefore in an increase of  $M_{\perp}$  with increasing  $\omega_c$ . Parallel to the magnetic field the radius of the electron wave function also decreases with increasing  $\omega_c$  because of the electron-phonon interaction, which tries to restore the spherical symmetry. Consequently, the effective electron-phonon interaction parallel to the magnetic field will also increase with increasing  $\omega_c$ , and correspondingly  $M_{\parallel}$  also increases. From the intuitive picture one expects that the radius of the electron wave function decreases more rapidly in the direction perpendicular to the magnetic field than in the direction parallel to the magnetic field. The result is that  $M_{\perp}$  increases faster with the magnetic field than  $M_{\parallel}$ . Our numerical calculation (see Fig. 2) displays such a behavior if  $\omega_c/\omega_0 \ll 1$  [see also Eqs. (72a) and (72b) in paper I].

To understand the high magnetic field ( $\omega_c/\omega_0 \gg 1$ ) behavior of  $M_{\perp}$  we present the following tentative interpretation. First, consider the situation without electron-phonon interaction. Then, perpendicular to the magnetic field the electron behaves as a harmonic oscillator with frequency  $\omega_c$ . The phonons are also harmonic oscillators but with a different characteristic frequency  $\omega_0$ . When the electron-phonon interaction is switched on, the phonon oscillators will try to follow the electron oscillatory motion, resulting in the polarization cloud. If  $\omega_c/\omega_0 \gg 1$  the electron oscillates so rapidly that the phonon oscillators can no longer follow the electron motion, and the polarization cloud vanishes. In other words, for  $\omega_c/\omega_0 \gg 1$  the effective electron-phonon interaction decreases with increasing  $\omega_c$ . This means if  $\omega_c \rightarrow \infty$  then  $v_1 \rightarrow \omega_1$ , or  $M_{\perp} \rightarrow 1$ , as is apparent from Fig. 2.

To summarize, we note that in the direction perpendicular to the magnetic field two mutually opposing effects are operative. First, there is an increasing localization of the electron with increasing magnetic field which, for small magnetic fields ( $\omega_c/\omega_0 \ll 1$ ), accounts for the increase of the polaron masses  $M_{\perp}$  and  $M_{\parallel}$  with increasing  $\omega_c$ . Second, the magnetic field induces an oscillatory motion of the electron which, for high  $\omega_c$ , prevents the phonons from interacting in an efficient way with the electron. This results in a decrease of  $M_{\perp}$  with increasing  $\omega_c$ . Parallel to the magnetic field, no oscillatory motion is induced by the magnetic field, and thus  $M_{\parallel}$  keeps increasing for large magnetic fields.

The above intuitive explanation for the magnetic field behavior of  $M_{\perp}$  and  $M_{\parallel}$  can be made more explicit by a direct calculation of the induced polarization charge density. This is done in the Appendix.

The magnetization,<sup>18</sup>  $\mathcal{M} = \mathcal{M} - \mathcal{M}_e$ , and the susceptibility  $\tilde{\chi} = \chi - \chi_e$ , of the polaron referred to the electron magnetization ( $\mathcal{M}_e$ ) and the electron susceptibility ( $\chi_e$ ) are plotted, respectively, in Figs. 3(a) and 3(b) as a function of the magnetic field for the electron-phonon coupling constants  $\alpha = 1, 2$ , and 3. At  $T = 0$  the electron magnetization and susceptibility are given by<sup>19</sup>  $\mathcal{M}_e = -0.5$  and  $\chi_e = 0.0$  (dimensional units), respectively.

The derivatives  $\partial F/\partial \mathcal{H}$  and  $\partial^2 F/\partial \mathcal{H}^2$  are calculated numerically here because, except in limiting cases, the free energy  $F$  is only known numerically. Two independent numerical procedures were used to calculate the derivatives.

(1) A smoothing procedure<sup>20</sup> based on spline functions was used. This procedure gives, besides the free energy interpolated between the numerically calculated values, also the first and second derivatives of  $F$ .

(2) A procedure based on the method of differences.<sup>21</sup>

The magnetization of a free spinless electron is  $-0.5$ . As is apparent from Fig. 3(a) the electron-phonon interaction reduces the absolute value of  $\mathcal{M}$ , or  $|\mathcal{M}| < 0.5$  (but  $\mathcal{M} > -0.5$ ). This is understood as follows: For relatively small electric fields the effective-mass approximation for the polaron is valid<sup>16</sup> and thus  $\mathcal{M} = -0.5m/m^*$  ( $m^*$  is the polaron mass) in the zero magnetic field limit. Consequently, the contribution of the electron-phonon interaction to the zero magnetic field magnetization,  $\mathcal{M} = 0.5(1 - m/m^*)$ , increases with increasing  $\alpha$  (because  $m^*$  increases with increasing

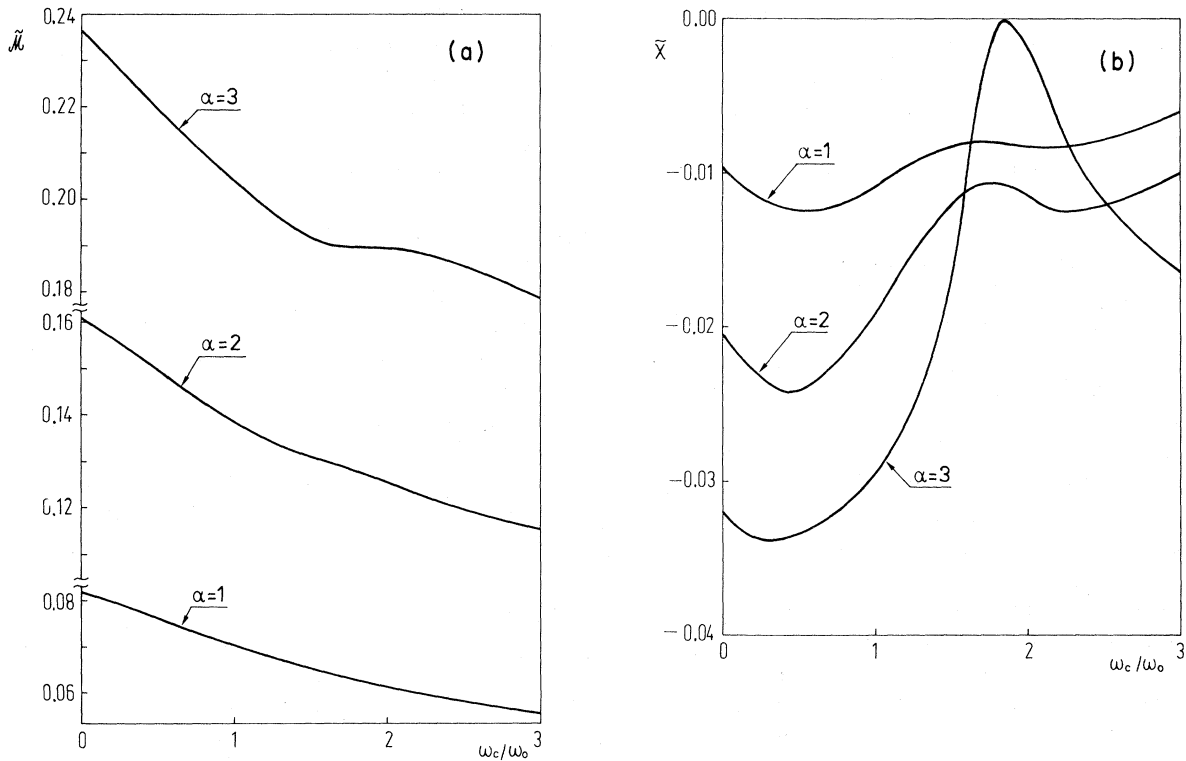


FIG. 3. (a) Magnetization  $\tilde{\mathcal{M}}$  and (b) susceptibility  $\tilde{\chi}$  of the polaron, shifted, respectively, with the free-electron values  $-0.5$  and  $0.0$  for  $\alpha=1,2,3$  and zero temperature. Thus  $\tilde{\mathcal{M}}$  and  $\tilde{\chi}$  are entirely a consequence of the electron-phonon interaction.

$\alpha$ ). For small electron-phonon coupling and small magnetic fields this can also be demonstrated analytically. From Eqs. (67) and (73) of paper I one obtains for the electron-phonon contribution to the magnetization per polaron (for  $\alpha \ll 1$  and  $\omega_c/\omega_0 \ll 1$ )

$$\tilde{\mathcal{M}} = \frac{1}{12} \alpha [1 - \frac{1}{10} \omega_c + O(\omega_c^2)] - \frac{1}{729} \alpha^2 [1 + O(\omega_c)] + O(\alpha^3), \quad (1)$$

which results in the zero magnetic field values  $\tilde{\mathcal{M}} = 0.0820, 0.161,$  and  $0.238,$  respectively, for  $\alpha=1, 2,$  and  $3.$  Note that these values for  $\tilde{\mathcal{M}}$  agree very well with the numerical results [see Fig. 3(a)]. This is rather surprising because the derivation of Eq. (1) was restricted to  $\alpha \ll 1.$

The two regimes apparent in the curves for  $M_{\perp}$  (see Fig. 2) are also present in the magnetization curves [see Fig. 3(a)]. For high magnetic fields,  $\tilde{\mathcal{M}}$  decreases more slowly than for low magnetic fields. The transition region between the “low” and

“high” magnetic field behavior of  $\tilde{\mathcal{M}}$  is the same as the magnetic field region in which  $M_{\perp}$  exhibits its steepest decrease (see Fig. 2). In the high magnetic field limit  $\mathcal{M}$  tends to the free-electron value  $-0.5,$  or  $\tilde{\mathcal{M}} \rightarrow 0$  for  $\omega_c/\omega_0 \rightarrow \infty$  as is apparent from our numerical calculation [see Fig. 3(a)]. For small electron-phonon coupling this can also be shown analytically because in paper I we calculated the asymptotic form of the free energy for large magnetic fields [see Eq. (76) of paper I]. This results in the magnetization

$$\mathcal{M} = \frac{\alpha}{2\omega_c} + O((\ln \omega_c)/\omega_c^{3/2}). \quad (2)$$

The susceptibility curves [Fig. 3(b)] show two structures. For small  $\omega_c$  the susceptibility  $\tilde{\chi}$  decreases as a function of the magnetic field. A local minimum is reached for a magnetic field value such that  $\omega_c/\omega_0 < 1.$  The position of this minimum shifts to smaller magnetic fields with increasing electron phonon coupling. This minimum is typical for the weak- (intermediate-) coupling region. As will become apparent later on, for  $\alpha \geq 4$

no such local minimum appears for  $\omega_c/\omega_0 < 1$ . For increasing  $\omega_c$  the susceptibility reaches a local maximum at  $\omega_c/\omega_0 > 1$ . This maximum appears at the magnetic field value where the steepest decrease of  $M_1$  is found (see Fig. 2). With increasing electron-phonon interaction the maximum in the susceptibility becomes more pronounced, and furthermore, the position of the maximum shifts to higher magnetic field values. In the asymptotic limit of high magnetic fields, and for small electron-phonon coupling, the susceptibility becomes [see Eq. (76) of paper I]

$$\tilde{\chi} = -\frac{\alpha}{2\omega_c^2} + O((\ln\omega_c)/\omega_c^{5/2}). \quad (3)$$

### B. Comparison with other theories and the importance of the anisotropy in the effective electron-phonon interaction

In Table I and in Fig. 4 the polaron ground-state energies obtained by different theories are compared as a function of the magnetic field for several values of the electron-phonon coupling constant. The Rayleigh-Schrödinger perturbation theory (RSPT) expression derived by Larsen in Ref. 8 and the result of Lépine and Matz<sup>22</sup> and of the adiabatic theory of Evrard *et al.*<sup>23</sup> (EKD) have been evaluated numerically. Kartheuser and Negrete<sup>24</sup> (KN) used the adiabatic approximation to calculate the ground-state energy (and the longi-

TABLE I. For two values of the electron-phonon coupling constant,  $\alpha=1$  and  $\alpha=3$ , numerical results are presented for the polaron ground-state energy of the following theories: Evrard, Kartheuser, and Devreese ( $E_{EKD}$ ), Larsen's Rayleigh-Schrödinger perturbation theory ( $E_{RSPT}$ ), Lépine and Matz ( $E_{LM}$ ), and the present result for a symmetrical ( $E_{sy}$ ) and an anisotropic ( $E_{as}$ ) effective electron-phonon interaction. The mass of the Feynman polaron corresponding to the energy  $E_{sy}$  is given by  $(v/w)^2$ . In the case of an anisotropic effective interaction two masses can be defined, namely  $(v_{\perp}/w_{\perp})^2$  and  $(v_{\parallel}/w_{\parallel})^2$ .

$\omega_c/\omega_0$	$E_{EKD}$	$E_{RSPT}$	$E_{LM}$	$E_{sy}$	$(v/w)^2$	$E_{as}$	$(v_{\perp}/w_{\perp})^2$	$(v_{\parallel}/w_{\parallel})^2$
$\alpha=1$								
0.0	-0.231 64	-1.000 00	-1.000 00	-1.013 03	1.17	-1.013 03	1.17	1.17
0.2	-0.216 60	-0.916 48	-0.918 06	-0.929 18	1.18	-0.929 20	1.18	1.18
0.4	-0.178 79	-0.832 51	-0.835 45	-0.844 90	1.19	-0.844 92	1.20	1.19
0.6	-0.127 58	-0.748 04	-0.752 09	-0.760 12	1.20	-0.760 15	1.21	1.21
0.8	-0.068 06	-0.663 02	-0.667 99	-0.674 84	1.21	-0.674 88	1.22	1.22
1.0	-0.002 87	-0.577 47	-0.583 17	-0.589 07	1.22	-0.589 14	1.21	1.23
1.2	0.066 45	-0.491 40	-0.497 69	-0.502 80	1.23	-0.503 00	1.16	1.25
1.4	0.138 91	-0.404 83	-0.411 58	-0.416 09	1.23	-0.416 48	1.13	1.26
1.6	0.213 88	-0.317 78	-0.324 91	-0.328 94	1.24	-0.329 57	1.11	1.28
1.8	0.290 88	-0.230 29	-0.237 71	-0.241 37	1.24	-0.242 32	1.09	1.30
2.0	0.369 58	-0.142 37	-0.150 03	-0.153 41	1.25	-0.154 42	1.05	1.33
3.0	0.781 14	0.302 71	0.294 48	0.291 35	1.27	0.288 06	1.04	1.39
5.0	1.6552	1.2132	1.2051	1.1995	1.35	1.1930	1.02	1.46
10.0	3.9589	3.5547	3.5479	3.5298	1.71	3.5201	1.00	1.74
$\alpha=3$								
0.0	-1.346	-3.000	-3.000	-3.133	1.79	-3.133	1.79	1.79
0.2	-1.343	-2.949	-2.978	-3.080	1.86	-3.080	1.85	1.84
0.4	-1.333	-2.898	-2.943	-3.025	1.92	-3.025	1.92	1.91
0.6	-1.316	-2.844	-2.900	-2.969	1.98	-2.969	1.98	1.98
0.8	-1.293	-2.789	-2.853	-2.912	2.03	-2.912	2.02	2.04
1.0	-1.265	-2.732	-2.803	-2.853	2.09	-2.853	2.04	2.11
1.2	-1.232	-2.674	-2.749	-2.793	2.14	-2.793	2.02	2.18
1.4	-1.195	-2.615	-2.692	-2.732	2.18	-2.732	1.93	2.25
1.6	-1.154	-2.553	-2.633	-2.669	2.22	-2.671	1.75	2.32
1.8	-1.110	-2.491	-2.572	-2.606	2.26	-2.609	1.52	2.39
2.0	-1.062	-2.427	-2.510	-2.542	2.30	-2.546	1.37	2.47
3.0	-0.789 4	-2.092	-2.179	-2.207	2.44	-2.231	1.11	3.02
5.0	-0.130 1	-1.360	-1.455	-1.490	2.39	-1.558	1.05	4.25
10.0	1.817	0.6640	0.5264	0.4575	4.29	0.314 1	1.01	7.20

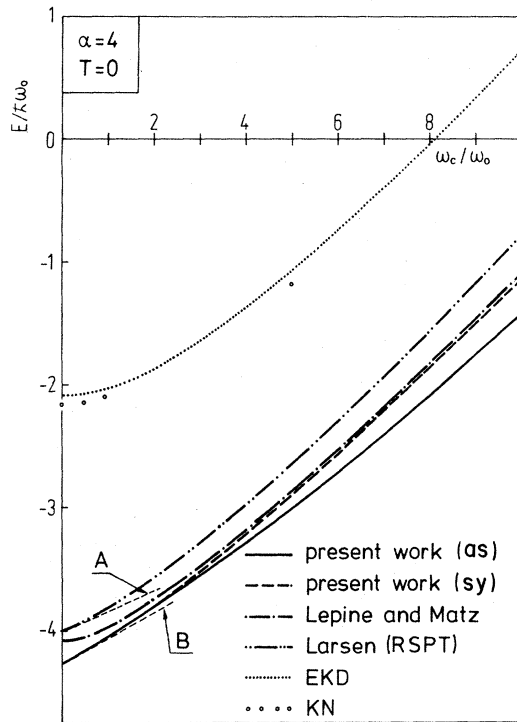


FIG. 4. Comparison between the polaron ground-state energy of different polaron theories for  $\alpha=4$  and zero temperature. We compared the results of Kartheuser and Negrete (KN, Ref. 24), Evrard, Kartheuser, and Devreese (EKD, Ref. 23), Larsen's Rayleigh-Schrödinger perturbation calculation (RSPT, Ref. 8), Lépine and Matz (Ref. 22), and the present result with a symmetrical (sy) and an anisotropic (as) effective electron-phonon interaction.

tudinal polaron mass) of a polaron in a magnetic field. They obtained lower results than EKD because correlation effects between the electron and the phonons were taken into account.

To investigate the importance of the anisotropy in the effective electron-phonon interaction we also calculated the polaron ground-state energy in the case of a symmetrical effective electron-phonon interaction. For that purpose a numerical variational calculation was performed using Eq. (60) of paper I with  $v=v_{\perp}=v_{\parallel}$  and  $w=w_{\perp}=w_{\parallel}$ . Only two, rather than four, variational parameters then remain. The results obtained with the symmetrical effective electron-phonon interaction are indicated with the symbol sy, those for the anisotropic effective electron-phonon interaction with the symbol as. For  $\alpha=1$  and 3 the results are tabulated (see Table I), while for  $\alpha=4$  where the differences between the different theories become quite large they are plotted (see Fig. 4). The corresponding re-

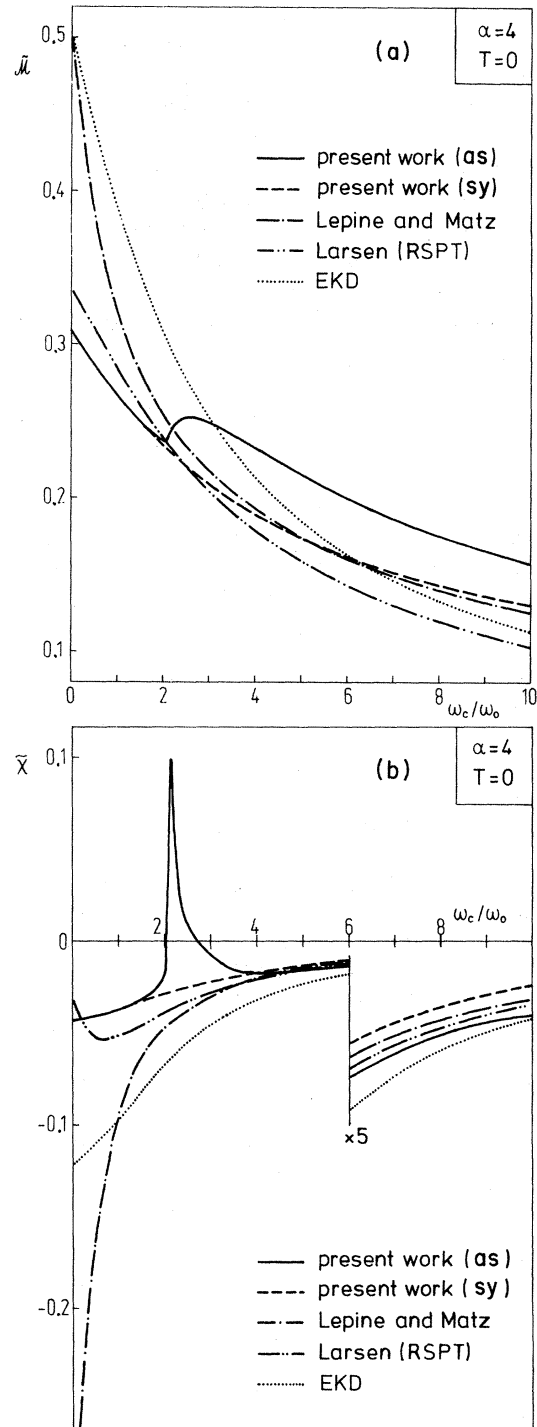


FIG. 5. Same as Fig. 4 but now we compared (a) magnetization and (b) susceptibility of the different theories.

sults for the magnetization and susceptibility for  $\alpha=4$  and  $T=0$  are plotted in Figs. 5(a) and 5(b).

From the numerical results presented in Table I and in Figs. 4, 5(a), and 5(b) we can conclude the

following.

(1) The large difference between the adiabatic theories<sup>23,24</sup> and the other approaches presented in Table I and in Fig. 4 are understood as follows. In the adiabatic theories only *one* trial wave function is used, while the other approaches use of a complete spectrum, and consequently a *complete set* of wave functions, to simulate the electron motion. Note that the region of numerical validity of Refs. 23 and 24 is limited to large magnetic fields ( $\omega_c/\omega_0 > 1$ ) and small and intermediate values of the electron-phonon coupling. However, the main significance of Ref. 23 is methodological. Furthermore, in Ref. 23 the rigorous asymptotic form for the polaron ground-state energy for  $\omega_c/\omega_0 \gg 1$  and  $\alpha \ll 1$  was obtained.

(2) The present result gives the lowest values for the ground-state energy of a polaron in a magnetic field obtained so far. Only for zero magnetic field have Larsen<sup>25</sup> and Adamowski *et al.*<sup>26</sup> obtained results that are slightly lower. Note that the difference between the polaron ground-state energy obtained with a symmetrical effective electron-phonon interaction ( $E_{sy}$ ) and the polaron ground-state energy obtained with the anisotropic effective interaction ( $E_{as}$ ) is very small for  $\omega_c/\omega_0 < 1$ . The same is true for the magnetization and the susceptibility of the symmetrical and anisotropic effective electron-phonon interaction. This is because, as we already noted,  $M_{\perp} = (v_{\perp}/w_{\perp})^2$  and  $M_{\parallel} = (v_{\parallel}/w_{\parallel})^2$  are nearly the same for  $\omega_c/\omega_0 < 1$  (see Fig. 2 and Table I).

(3) For the intermediate-coupling region the small magnetic field behavior of the ground-state energy of the various theories differs strongly. This is apparent from Fig. 4. For example, the small magnetic field behavior of the present result,  $E_{as}$  and  $E_{sy}$ , is given by (curve B in Fig. 4)

$$E_F(\alpha; v, w) + \frac{1}{2} \frac{\omega_c}{m_H} + O(\omega_c^2) \quad (4)$$

with  $E_F$  the Feynman<sup>2</sup> polaron ground-state energy and  $m_H$  the polaron magnetic mass (see Fig. 4 of paper I). The analytic expression for  $m_H$  has been given in Ref. 27. For  $\alpha=4$  one has  $E_F = -4.256$  and  $m_H = 2.58$ . The RSPT result, as obtained by Larsen,<sup>8</sup> gives (curve A in Fig. 4)

$$E_L(\omega_c) = -\alpha + \frac{1}{2} \omega_c(1 - \alpha/6) + O(\omega_c^2) \quad (5)$$

from which we obtain the perturbation result for the polaron mass:  $1/(1 - \alpha/6)$ . For  $\alpha=4$  one has  $1/(1 - \alpha/6) = 3$ . The ground-state energy of the Lépine-Matz approximation and the adiabatic

theories EKD and KN do not have such a linear term in the magnetic field [see Figs. 4 and 5(a)]. The first nonzero correction term is quadratic in  $\omega_c$ . Such a small magnetic field behavior for the polaron ground-state energy is unrealistic. Indeed from the effective-mass approximation, which is valid<sup>16</sup> for  $\omega_c/\omega_0 \ll 1$  and all  $\alpha$ , one obtains the following linear magnetic field correction to the polaron ground-state energy:  $\frac{1}{2} \omega_c/m^*$ , with  $m^*$  the polaron mass. One can show that the Lépine-Matz ground-state energy contains a term linear in  $\omega_c$  if  $\alpha < 3.8$ . It should be noted that EKD and KN are high-field approximations and are, in principle, not applicable in the small magnetic field region.

(4) For small magnetic fields ( $\omega_c/\omega_0 < 1$ ) the difference between the ground-state energy of the Lépine-Matz approximation and that obtained here decreases with increasing magnetic field strength. However, when the anisotropy in the effective electron-phonon interaction starts to become important (i.e., for  $\omega_c/\omega_0 > 1$ ), the difference between  $E_{as}$  and  $E_{LM}$  and between  $E_{as}$  and  $E_{sy}$  increases with increasing  $\omega_c$  (see Table I and Fig. 4). Note that for high magnetic field values the Lépine-Matz approximation to the polaron ground-state energy, the magnetization, and the susceptibility is close to the result of the present work, in the case of a symmetrical effective electron-phonon interaction [see Figs. 4, 5(a), and 5(b)].

(5) The incorporation of the anisotropy in the effective electron-phonon interaction drastically changes the behavior of the susceptibility [see Fig. 5(b)]. For example, the peak structure in  $\chi$  is entirely a consequence of this anisotropy [compare the curves  $as$  and  $sy$  in Fig. 5(b)]. This observation leads to the conclusion that the detailed simulation of the electron motion, by the trial action, is of crucial importance. Note that the susceptibility as obtained from Larsen's RSPT calculation shows a minimum. As mentioned before, this is a consequence of the weak-coupling nature of RSPT.

### III. STUDY OF THE PHASE TRANSITION OF AN IDEAL POLARON GAS IN A MAGNETIC FIELD (ZERO TEMPERATURE)

It should be noted that for each value of  $\alpha$  and  $\omega_c$  (here we take  $T=0$ ) we must find the minimum of the expression for the polaron ground-state energy [see Eq. (59a) of paper I] in the four-dimensional parameter space

$(v_{\perp}, w_{\perp}, v_{\parallel}, w_{\parallel})$ . A numerical calculation shows that this energy exhibits one minimum if  $\alpha \leq 2.4$ . This is true for all magnetic fields if  $T=0$ . In this coupling region ( $\alpha \leq 2.4$ ) the polaron state evolves continuously from the small to the large magnetic field behavior [e.g., see Fig. 2 and Figs. 3(a) and 3(b)].

If  $\alpha > 4.2$ , and for a certain range of magnetic field values the polaron ground-state energy has two local minima in the four-dimensional space of variational parameters. This is illustrated in Fig. 6 for the special case  $\alpha=5$ . For simplicity we

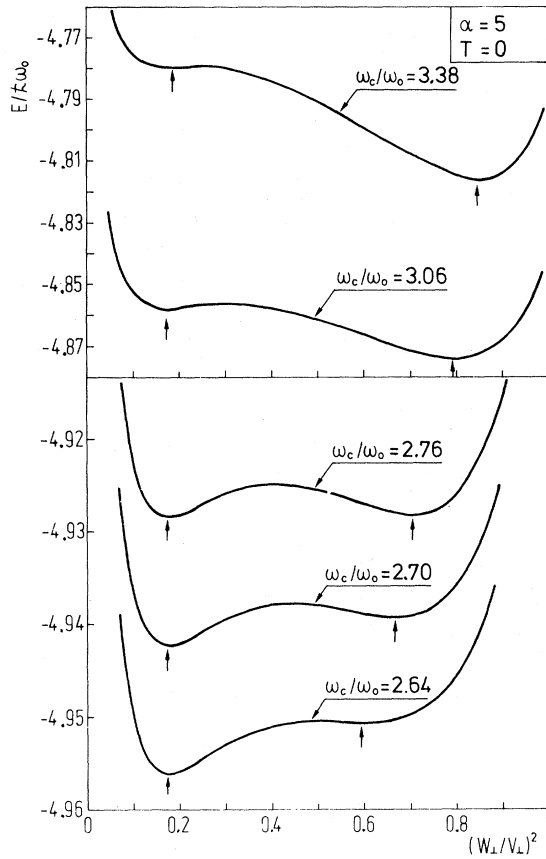


FIG. 6. Polaron ground-state energy as function of the inverse of the mass  $M_{\perp}=(v_{\perp}/w_{\perp})^2$  for  $\alpha=5$ , zero temperature, and for different values of the magnetic field. The energy was calculated along a straight line in the four-dimensional parameter space. This line was defined by  $v_{\perp}=aw_{\perp}+b$  and  $(v_{\parallel}, w_{\parallel})$  was taken fixed. The set of constants  $(a, b, v_{\parallel}, w_{\parallel})$  are, respectively, equal to (0.865, 3.03, 4.17, 1.73) for  $\omega_c/\omega_0=2.64$ , (0.876, 3.03, 4.17, 1.71) for  $\omega_c/\omega_0=2.70$ , (0.883, 3.03, 4.17, 1.70) for  $\omega_c/\omega_0=2.76$ , (0.901, 3.09, 4.21, 1.66) for  $\omega_c/\omega_0=3.06$ , and (0.915, 3.15, 4.26, 1.63) for  $\omega_c/\omega_0=3.38$ . The arrows pointing upward indicate the position of the local minima.

present in Fig. 6 only the energy values as calculated along a certain line in the four-dimensional parameter space. This straight line is defined by  $v_{\perp}=aw_{\perp}+b$  and  $(v_{\parallel}, w_{\parallel})$ , where the values for  $a$ ,  $b$ ,  $v_{\parallel}$ , and  $w_{\parallel}$  are chosen such that it connects both minima approximately. The resulting energy is then plotted as function of the inverse of the Feynman polaron mass perpendicular to the magnetic field, namely  $1/M_{\perp}=(w_{\perp}/v_{\perp})^2$ . For  $\omega_c/\omega_0 < 2.64$  ( $\alpha=5$ ) the polaron ground-state energy has only one local minimum in the four-dimensional space of variational parameters. With increasing magnetic field a second local minimum appears at a smaller value of  $M_{\perp}$  (see Fig. 6). As is apparent from Fig. 6 the second local minimum becomes more and more pronounced with increasing magnetic field strength. For  $\omega_c/\omega_0 < 2.76$  the minimum corresponding to the largest  $M_{\perp}$  value is the lowest one, and this minimum will correspond to the stable polaron state, while the second minimum corresponds to the metastable state. At  $\omega_c/\omega_0=2.76$  the energy corresponding to both minima are the same. For still larger magnetic field values the local minimum at the smallest  $M_{\perp}$  value is the lowest one and will correspond to the stable polaron state, while the other minimum now characterizes the metastable state. This means that, for a polaron in a magnetic field, the polaron state changes discontinuously at  $\omega_c/\omega_0=2.76$  (for  $\alpha=5$  and  $T=0$ ). This transition is a first-order transition. At the transition point the mass  $M_{\perp}$  changes discontinuously and consequently also the effective interaction between the electron and the phonons.

Now we examine the electron-phonon coupling region around  $\alpha=4.2$  as function of the magnetic field. In Fig. 7 the masses of the Feynman polaron are plotted as function of the magnetic field around the onset of the phase transition. Two main features are apparent from Fig. 7.

(1) The small and high magnetic field behavior of the polaron are connected in a continuous way if  $\alpha < 4.2$  (see also Fig. 2). There is a finite transition width, or there is a *transition region*. For  $\alpha < 4.2$  the transition occurs at a well-defined *transition point*. The transition region for  $\alpha < 4.2$ , or the transition point if  $\alpha \geq 4.2$ , shifts to larger  $\omega_c$  values with increasing electron-phonon coupling. The effect of the transition on  $M_{\perp}$ , and to a lesser extent on  $M_{\parallel}$ , becomes larger with increasing  $\alpha$ .

(2) For  $\alpha > 4.2$  the Feynman polaron mass parallel to the magnetic field  $M_{\parallel}$  also exhibits a jump, which, however, is much smaller than the jump in

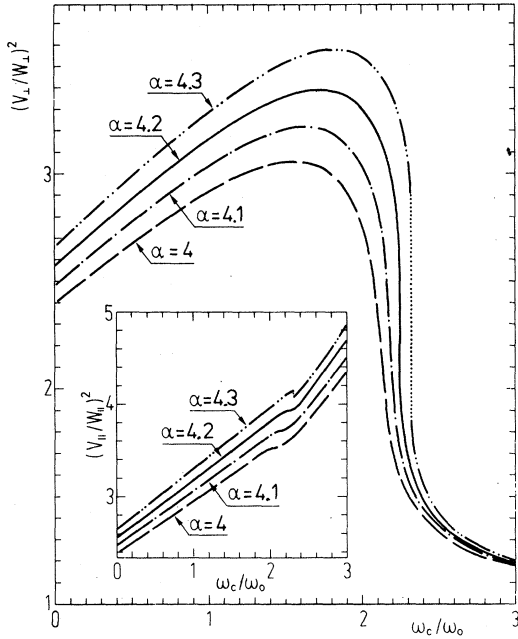


FIG. 7. Mass of the Feynman polaron in the direction perpendicular,  $M_{\perp}=(v_{\perp}/w_{\perp})^2$ , and parallel,  $M_{\parallel}=(v_{\parallel}/w_{\parallel})^2$ , to the magnetic field (inset of figure), for  $\alpha=4, 4.1, 4.2, 4.3$ . The temperature is equal to zero.

$M_{\perp}$ . For magnetic fields above the transition the slope of  $M_{\parallel}$  is larger compared to the slope of  $M_{\perp}$  before the transition. Furthermore, note that for  $\omega_c > \omega_0$  the anisotropy in the effective electron-phonon interaction starts to increase drastically with increasing magnetic field as is apparent from Fig. 7.

In Figs. 8(a) and 8(b), respectively, the magnetization  $\tilde{\mathcal{M}}$  and the susceptibility  $\tilde{\chi}$  of the polaron (referred to their value at  $\alpha=0$ ) are plotted in the neighborhood of the transition region. Figure 8(a) shows that the electron-phonon contribution to the magnetization is largest for the polaron state with smallest mass  $M_{\perp}$ . For large magnetic field values the magnetization asymptotically decreases to zero. Note that for  $\alpha \leq 4.2$  the magnetization is a continuous function while for  $\alpha > 4.2$  it has a discontinuity at a certain critical magnetic field, which indicates that a first-order phase transition<sup>28</sup> takes place.

The peak in the susceptibility, which was already present in Fig. 3(b), becomes more pronounced as  $\alpha$  increases. At  $\alpha=4.20 \pm 0.01$  the susceptibility diverges at  $\omega_c/\omega_0=2.24 \pm 0.01$ , which implies that a second-order phase transition takes place (because in this point the magnetization  $\mathcal{M}$  is still continuous). For  $\alpha > 4.2$  the susceptibility has a discontinuity

for the same magnetic field as  $\tilde{\mathcal{M}}$ ,  $M_{\perp}$ , and  $M_{\parallel}$ .

For larger electron-phonon coupling,  $\alpha=5, 6$ , and 7, we plotted the mass of the Feynman polaron perpendicular [Fig. 9(a)] and parallel [Fig. 9(b)] to the magnetic field, the magnetization [Fig. 10(a)], and the susceptibility [Fig. 10(b)]. The solid curves in these figures indicate the value in the stable polaron state, while the dashed curves give the value in the metastable state. For  $M_{\perp}$ ,  $M_{\parallel}$ , and  $\tilde{\mathcal{M}}$  the different effects around the phase-transition point become more pronounced for increasing  $\alpha$ . In contrast the jump in the susceptibility at the phase-transition point becomes smaller with increasing  $\alpha$ .

Now we can construct a *phase diagram* of the ideal polaron gas as a function of the physical parameters, which for  $T=0$  are the magnetic field  $\omega_c/\omega_0$  and the electron-phonon coupling strength  $\alpha$ . Such a plot has already been reported in Ref. 6. It turns out to be more interesting to plot the points, at which a discontinuous change takes place, in a  $1/\alpha - \omega_0/\omega_c$  plane. An elementary version of such a plot has been presented in Ref. 29. In Fig. 11 we have extended this plot to higher  $\alpha$  and  $\omega_c$  values. The solid curve in Fig. 11 represents the points at which a first-order phase transition takes place. The curve ends at the point ( $\alpha=4.20 \pm 0.01, \omega_c/\omega_0=2.24 \pm 0.01$ ). This point, at which a second-order phase transition takes place [see Figs. 8(a) and 8(b)], is the critical point.<sup>28</sup> In the region between the dashed curves metastable states can exist.

In what follows, the difference between the weak- and strong-coupling behavior of the phase transition is discussed. For small  $\alpha$ , the polarization cloud will follow the electron adiabatically (see, e.g., the discussion of Allcock in Ref. 30 on the dynamic or high-frequency approximation). For magnetic fields such that  $\omega_c < \omega_0$  the polarization cloud will still be able to follow the electron. However, for  $\omega_c > \omega_0$  the electron oscillates so rapidly that the phonons can no longer follow the electron adiabatically. In the direction perpendicular to the magnetic field the polarization will then diminish, which gives rise to a decreasing polaron mass  $M_{\perp}$  with increasing magnetic field. This *stripping* of the polaron occurs for  $\omega_c/\omega_0 \sim 1$ . It is a continuous process as function of the magnetic field (see Fig. 2).

For large  $\alpha$  we are in a totally different situation. The electron will now follow the polarization changes adiabatically. The electron moves in a self-induced potential well, which is built up by the

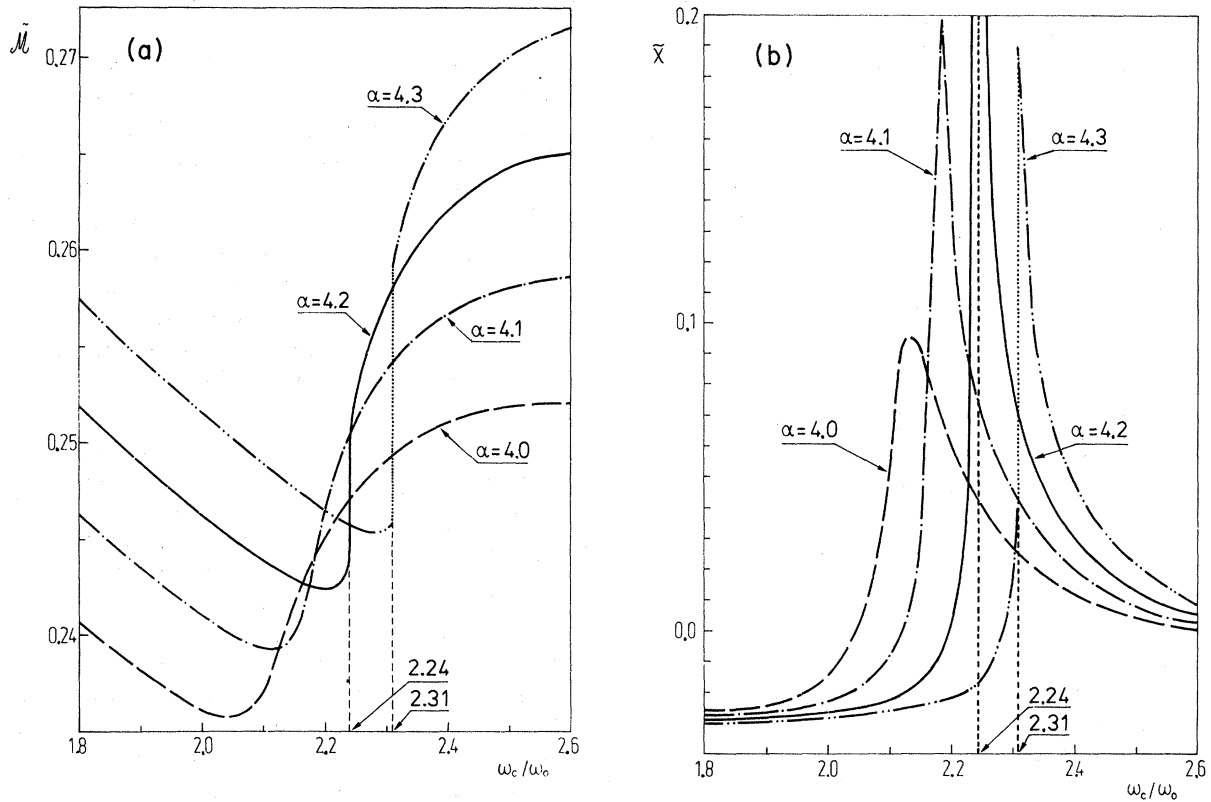


FIG. 8. (a) Magnetization and (b) susceptibility of the polaron (referred to the value of a free electron in a magnetic field) around the transition region. For  $\alpha=4.20\pm 0.01$  the susceptibility diverges at  $\omega_c/\omega_0=2.24\pm 0.01$ .

highly correlated motion of electron and phonons (the latter can be treated as almost static<sup>30</sup>). The correlated electron-phonon motion induces an electron oscillatory motion with a characteristic frequency  $\nu$  that is proportional to  $\alpha^2\omega_0$ . The magnetic field, on the other hand, imposes an oscillatory motion with frequency  $\omega_c$ . As long as  $\omega_c < \nu$ , the electron can still move in a correlated way with the phonons, and this implies that  $M_{\parallel} \approx M_{\perp}$ . An increase of the magnetic field so that  $\omega_c > \nu$  will destroy the correlated electron-phonon motion. The electron oscillatory motion induced by the magnetic field is so rapid that there no longer exists any correlation between the electron and the phonons in the direction perpendicular to the magnetic field. The electron-phonon interaction becomes inefficient, and a reduction of the polaron mass  $M_{\perp}$  results, i.e.,  $M_{\parallel} \gg M_{\perp} \sim 1$ . The transition to this symmetry-breaking state occurs when  $\omega_c \sim \nu$  or  $\omega_c/\omega_0 \sim \alpha^2$ . For large  $\alpha$ , the line of first-order phase transition behaves like  $1/\alpha \sim (\omega_0/\omega_c)^{1/2}$ , which is in agreement with Fig. 11.

Until now nothing has been said about the order

parameter. Because there are four variational parameters in the problem, it is not trivial to define one order parameter. Nevertheless, we will suggest one. Note that in this section  $M_{\perp}$  has been considered as the crucial parameter in identifying the phase transition. The mass of the Feynman polaron perpendicular to the magnetic field is a measure for the effective electron-phonon interaction. The magnitude of the discontinuity in  $M_{\perp}$  indicates how drastic the effect of the phase transition is on the polaron state. At the transition point we define the quantity  $\Delta(1/M_{\perp})$  as the difference between  $1/M_{\perp}$  calculated in the symmetry-breaking polaron state with  $M_{\parallel} \gg M_{\perp} \sim 1$  and  $1/M_{\perp}$  calculated in the normal polaron state with  $M_{\perp} \approx M_{\parallel}$ . The quantity  $\Delta(1/M_{\perp})$  is plotted in Fig. 12 as function of  $4.2/\alpha$ . For illustrative purposes we plotted the order parameter in the case of an ideal Bose gas (dashed-dotted curve) and in the case of the three-dimensional Ising model (dashed curve). For an ideal Bose gas the order parameter is given by  $N_0/N = 1 - (T/T_c)^{3/2}$ , with  $N_0/N$  the relative number of condensed parti-

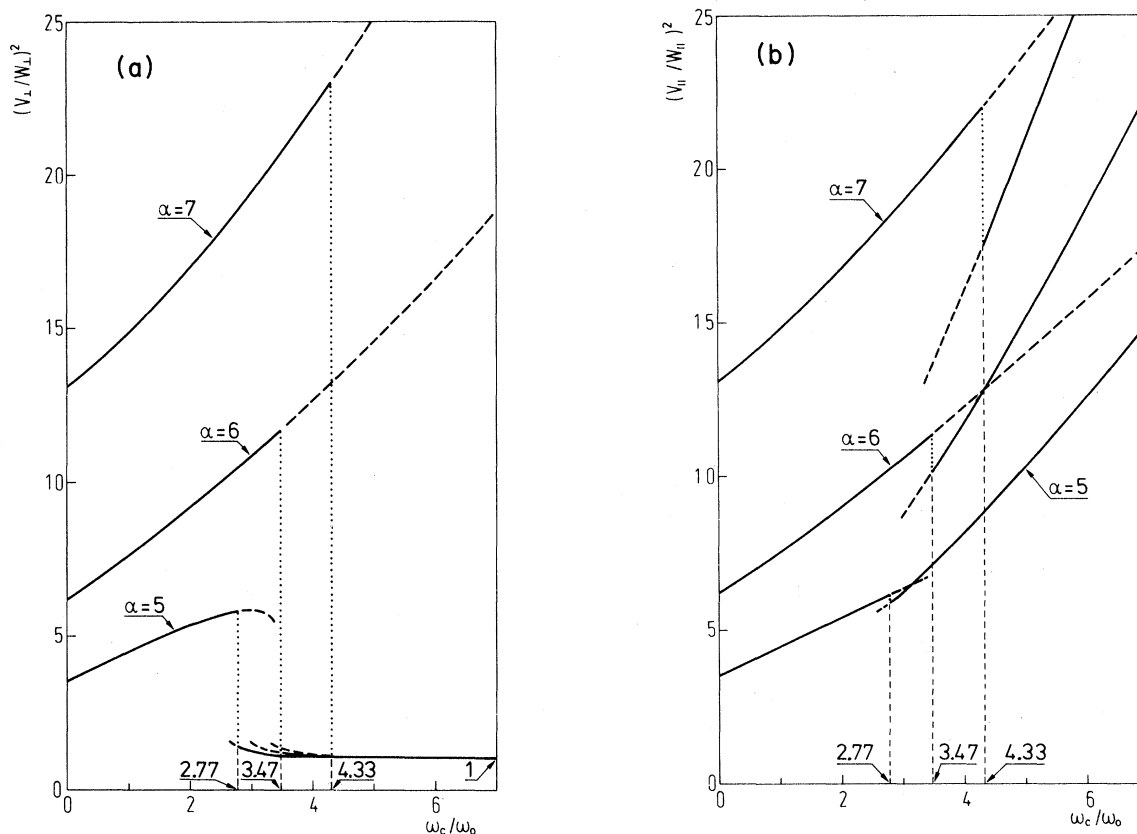


FIG. 9. Masses of the Feynman polaron (a) perpendicular and (b) parallel to the magnetic field for  $\alpha = 5, 6, 7$  and  $T = 0$ .

cles and  $T/T_c$  the temperature  $T_c$  (see, e.g., Ref. 31, p. 248). As is well known the Ising model, treated in the molecular field approximation (see, e.g., Ref. 31, p. 302), leads to the following equation for the order parameter:

$$X = \tanh(XT_c/T),$$

with  $X = M_s / M_\infty$ , where  $M_s$  is the spontaneous magnetization and  $M_\infty$  the magnetization at  $T = 0$ .

Two remarks are in order. First, in the above analogy between the present order parameter and the order parameter for the ideal Bose gas or the Ising model,  $4.2/\alpha$  corresponds formally to  $T/T_c$ . This is in agreement with earlier suggestions to interpret formally  $1/\alpha$  as an effective temperature if one is dealing with phase transitions in the polaron problem.<sup>12,14</sup> Second, the behavior of the order parameter around the critical point defines a critical exponent<sup>32</sup>  $\beta$  resulting from  $\Delta(1/M_1) \sim (1 - 4.2/\alpha)^\beta$ . The present numerical analysis gives  $\beta = 0.63 \pm 0.01$ . Owing to numerical accuracy

problems it was not possible to determine the other critical exponents, which are connected, e.g., with the susceptibility and the specific heat.

#### IV. THE TEMPERATURE DEPENDENCE OF THE POLARON PROPERTIES AT ZERO MAGNETIC FIELD

In the absence of a magnetic field the effective electron-phonon interaction is isotropic and thus  $v_\perp = v_\parallel = v$ ,  $w_\perp = w_\parallel = w$ , which implies  $M_\perp = M_\parallel = M = (v/w)^2$ . The temperature dependence of the polaron mass  $M$  has been studied by Osaka<sup>33</sup> in the limit of small electron-phonon coupling. We have extended this calculation to arbitrary  $\alpha$  (see Fig. 13). For low temperature the effective mass  $M$  increases with  $T$ . As explained in Ref. 33 this increase can be attributed to the nonparabolicity of the polaron conduction band. At higher temperature the uncorrelated motion of the phonons becomes an important factor. It results in a decrease

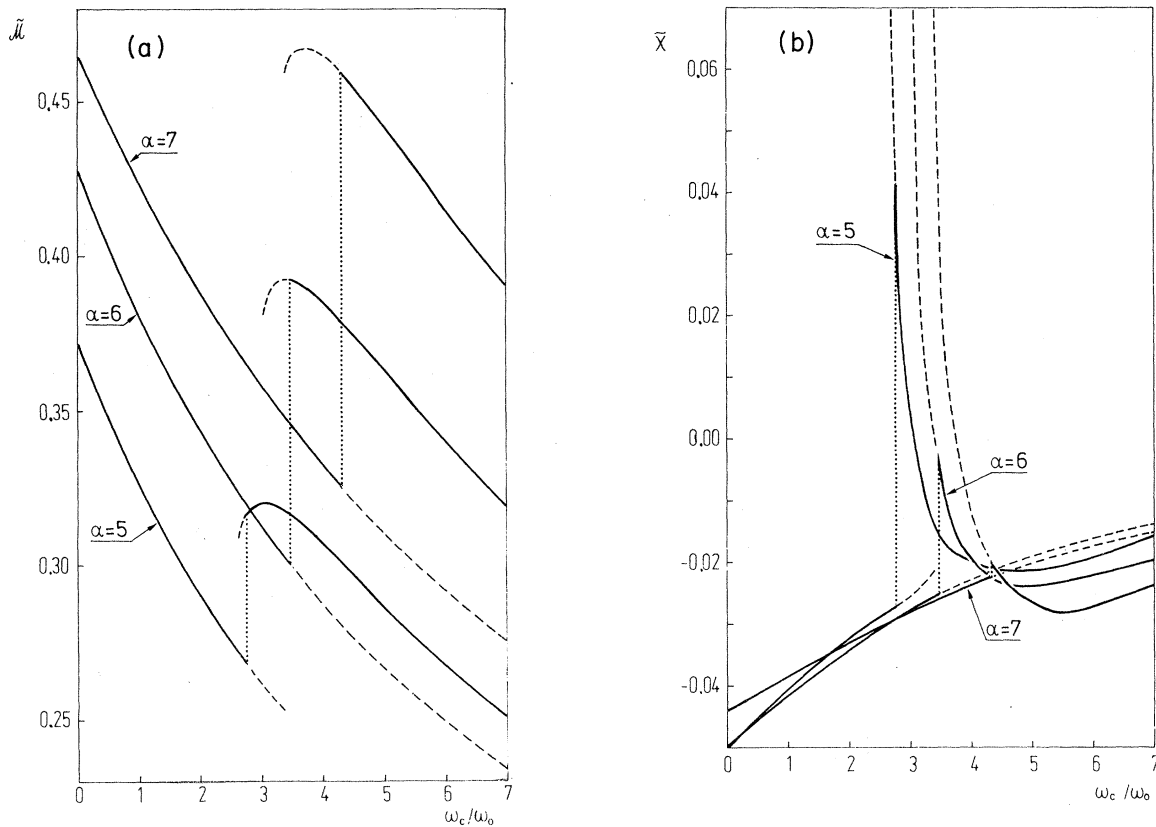


FIG. 10. Same as Fig. 3 but now for large electron-phonon coupling, namely,  $\alpha=5,6,7$ .

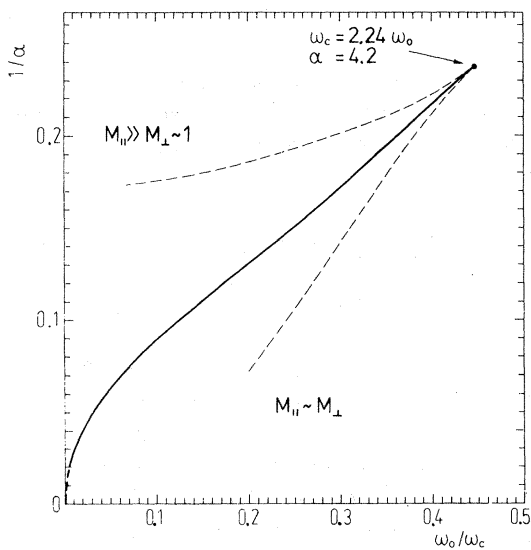


FIG. 11. Phase diagram for the polaron ground state [solid curve, which is extrapolated to very large  $\alpha$  and very large  $\omega_c$  values (thick-dashed curve)]. Metastable states can exist between the dashed curves.  $M_{\perp}=(v_{\perp}/\omega_{\perp})^2$  and  $M_{\parallel}=(v_{\parallel}/\omega_{\parallel})^2$  are the masses of the Feynman polaron, respectively, perpendicular and parallel to the magnetic field.

of the coherence between the electron motion and the motion of the phonons, i.e., the electron-phonon interaction becomes less effective, which results in a decrease of  $M$ . Note that the general trend of the temperature dependence of the polaron

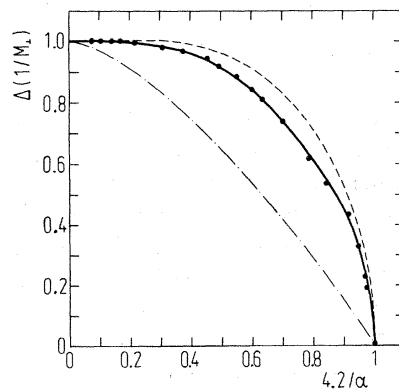


FIG. 12. Order parameter  $\Delta(1/M_{\perp})$  as function of the inverse of the electron-phonon coupling constant. For comparison the order parameter of a Bose gas (dashed-dotted curve) and of the Ising model (dashed curve) are shown.

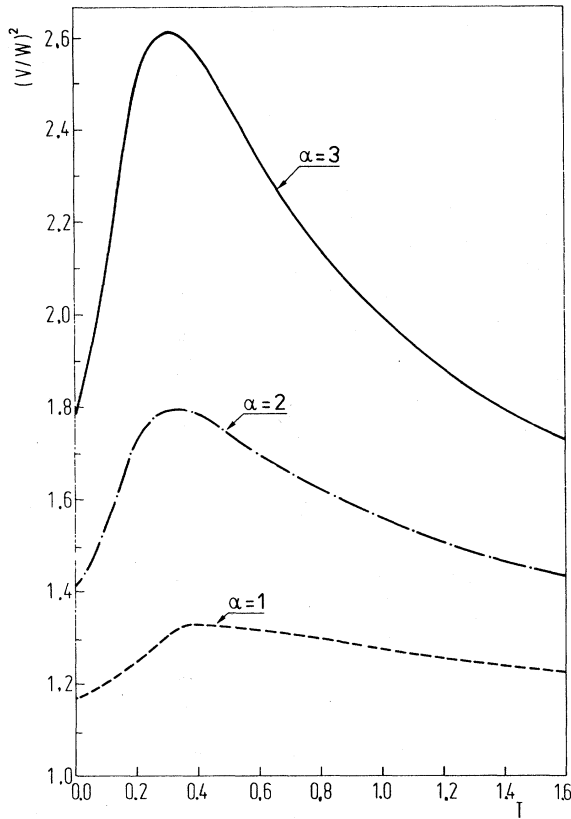


FIG. 13. Mass of the Feynman polaron  $M=(v/w)^2$  as function of the temperature for different values of the electron-phonon coupling and in the absence of external fields.

mass is almost independent of  $\alpha$  (see Fig. 13). With increasing  $\alpha$  one finds that  $M$  increases more rapidly for small  $T$  and decreased faster at higher  $T$ ; the peak structure in the mass-temperature curve becomes more pronounced. The position of the peak shifts to smaller  $T$  values with increasing electron-phonon coupling, namely for  $\alpha=1, 3, 5, 7,$  and  $9$  the peak is located, respectively, at<sup>34</sup>  $T=0.38, 0.31, 0.27, 0.24,$  and  $0.23$  (numerical accuracy  $\pm 0.01$ ). In the asymptotic limit  $\alpha \rightarrow \infty$  the peak seems to occur at  $T=0.20$ .

The contribution of the electron-phonon interaction to the polaron internal energy is plotted in Fig. 14(a) as a function of temperature for different values of  $\alpha$ . Note that  $\tilde{E}=E-E_e$ , with  $E=\partial(\beta F)/\partial\beta$  the polaron internal energy and  $E_e$  the free-electron energy. In the zero-temperature limit the internal energy  $E$  ( $=\tilde{E}$ ) equals the polaron ground-state energy. For nonzero temperature the polaron has a finite amplitude for occupation of higher excited polaron states, and as a

consequence  $E$  (or  $\tilde{E}$ ) has to be interpreted as an average energy. For small electron-phonon coupling and low temperature the internal energy is analytically given by [use Eqs. (79) and (83) of paper I]

$$\tilde{E} = -\left[\alpha + \frac{1}{81}\alpha^2 + O(\alpha^3)\right] + \frac{1}{\beta^2}\left[\frac{9}{32}\alpha + O(\alpha^2)\right] + O(1/\beta^3). \quad (6)$$

Note that the low-temperature correction to  $\tilde{E}$  is quadratic in  $T$  ( $\beta=1/k_B T$ ); no term linear in  $T$  is present. Increasing the temperature increases  $E$  until it reaches a maximum. The position of this maximum shifts to smaller  $T$  values with increasing  $\alpha$ . For still higher temperatures the internal energy  $\tilde{E}$  starts to decrease. Analytically, we obtain for weak coupling the following high temperature limit [see Eq. (85) of paper I]:

$$\tilde{E} = -\frac{\alpha}{2} \left[ \frac{\pi}{\beta} \right]^{1/2} \left[ 1 + \frac{5}{48}\beta^2 + O(\beta^5) \right] + O(\alpha^2), \quad (7)$$

which shows that in the asymptotic limit  $T \rightarrow \infty$  the internal energy  $\tilde{E}$  diverges as the square root of  $T$ . Note that the free-electron energy [see Eq. (78) of paper I] is given by  $E_e=3/(2\beta)$ , which implies that the total polaron internal energy  $E$  will diverge like  $T$  in the considered asymptotic limit  $T \rightarrow \infty$ .

The effect of the electron-phonon interaction on the entropy is shown in Fig. 14(b), where  $\tilde{S}=S-S_e$  with  $S=-\partial F/\partial T$  the polaron entropy and  $S_e$  the free-electron entropy. For small electron-phonon coupling we obtain the following analytic expressions for the entropy<sup>34</sup> per polaron:

$$\tilde{S} = \frac{1}{4}\alpha \left[ 1 + \frac{16}{729}\alpha + O(\alpha^2) \right] + \frac{1}{\beta} \left[ \frac{9}{16}\alpha + O(\alpha^2) \right] + O(1/\beta^2) \quad (8)$$

in the low-temperature limit [use Eqs. (79) and (83) of paper I] and

$$\tilde{S} = \frac{1}{2}\alpha \sqrt{\pi} \sqrt{\beta} \left[ 1 - \frac{1}{32}\beta^2 + O(\beta^3) \right] + O(\alpha^2) \quad (9)$$

in the high-temperature limit [use Eq. (85) of paper I].

In Fig. 14(c) the effect of the electron-phonon interaction on the specific heat is plotted as a function of temperature for different values of the

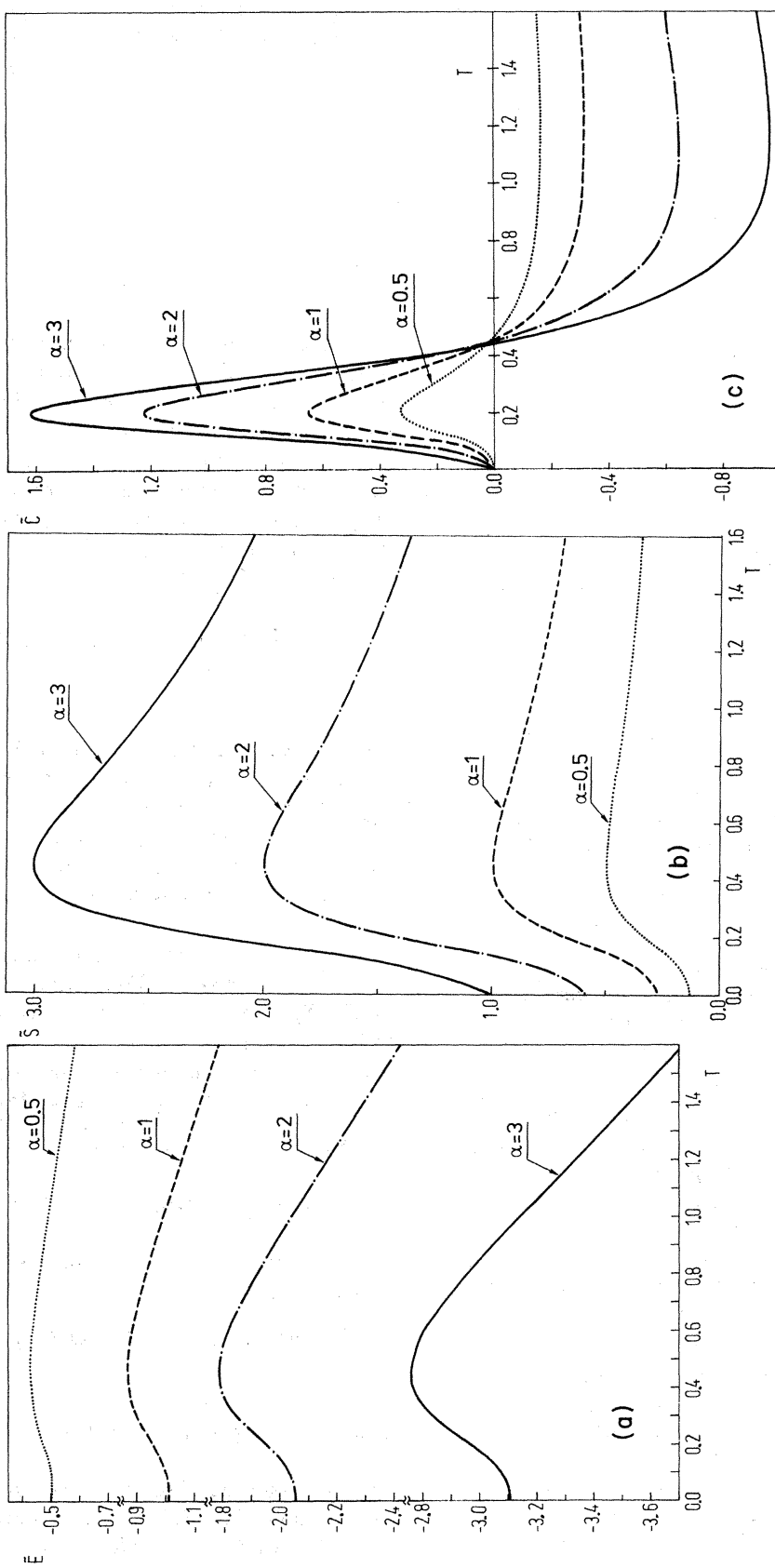


FIG. 14. Contribution of the electron-phonon interaction to (a) internal energy, (b) entropy, and (c) susceptibility as function of temperature and in the absence of external fields.

electron-phonon coupling strength. Note that  $\tilde{C} = C - C_e$  with  $C = -T\partial^2 F/\partial T^2$  the polaron specific heat and  $C_e = \frac{3}{2}$  the free-electron specific heat. As is apparent from Fig. 14(c), the specific heat exhibits a characteristic peak whose amplitude increases with  $\alpha$ . The position of this peak is located at the temperature<sup>34</sup>  $T = 0.20 \pm 0.01$  and is independent of the electron-phonon coupling strength. We have verified this numerically for values of  $\alpha$  between 0 and 10. Furthermore, the position of this peak does not seem to be very sensitive to the approximation used to calculate  $\tilde{C}$  (and thus to calculate  $F$ ). For example, for  $\alpha = 3$  we calculated the free energy using perturbation theory (this means  $v = w$  in the Feynman trial action) and found that the amplitude of the peak is 1.98, which compares to 1.61 for the variational result. The position of the peak remains at  $T = 0.20 \pm 0.01$ . If the parameters  $v$  and  $w$  are varied slightly, e.g.,  $(v, w) = (4.0, 2.1)$  and  $(3.42, 2.56)$  the peak amplitude becomes, respectively, 1.31 and 1.97, while the peak position is still located at  $T = 0.20 \pm 0.01$ .

Increasing the lattice temperature above a certain value alters the sign of the contribution of the electron-phonon interaction to the specific heat. The temperature at which  $\tilde{C}$  equals zero decreases only slightly with increasing  $\alpha$ . For example, for  $\alpha = 1, 3, 5, 7,$  and  $9$  the specific heat  $\tilde{C}$  becomes zero, respectively, at the temperature  $T = 0.46, 0.45, 0.43, 0.41,$  and  $0.40$  (numerical accuracy  $\pm 0.01$ ). Above these temperatures  $\tilde{C}$  decreases to a minimum and for still larger temperature increases again to the asymptotic value zero.

The following expansions for the specific heat  $\tilde{C}$  are obtained in the small electron-phonon coupling limit. For low temperature one obtains [use Eqs. (79) of paper I]

$$\tilde{C} = \frac{9}{16} \frac{\alpha}{\beta} \left[ 1 + O\left(\frac{1}{\beta}\right) \right] + O(\alpha^2), \quad (10)$$

while for high temperature [use Eq. (85) of paper I]

$$\tilde{C} = -\alpha \frac{\sqrt{\pi}}{4} \sqrt{\beta} \left[ 1 - \frac{5}{16} \beta^2 + O(\beta^3) \right] + O(\alpha^2) \quad (11)$$

is found.

A striking feature of the temperature dependence of the polaron mass  $M$  and the thermodynamic quantities  $\tilde{E}$ ,  $\tilde{S}$ , and  $\tilde{C}$  is that the general form of those curves is not very sensitive to the value of  $\alpha$ . A typical example is the  $\alpha$  independence of the peak position in the  $\tilde{C}-T$  curve. This is why only figures have been presented here for  $\alpha$  between 0.5 and 3. For  $\alpha > 3$  no new features appear in the general form of the temperature dependence of  $M$ ,  $\tilde{E}$ ,  $\tilde{S}$ , and  $\tilde{C}$ . This is completely different compared to the magnetic field dependence of  $M$ ,  $\tilde{M}$ , and  $\tilde{\chi}$ , the behavior of which depend strongly on  $\alpha$ . This was most dramatically shown in Sec. III for  $\alpha > 4.2$ .

## V. COMBINED INFLUENCE OF TEMPERATURE AND A MAGNETIC FIELD ON THE PHASE TRANSITION

In the previous sections the effect of an external magnetic field and the effect of the temperature on the properties of the polaron have been studied separately. In this section we consider the combined effects of temperature and magnetic field on the behavior of polarons. The electron-phonon coupling strength will be fixed; as an example we take  $\alpha = 3$ . First, the properties of the polaron will be studied as a function of the magnetic field for different values of the temperature. Subsequently, the effect of the magnetic field on the temperature behavior of the polaron is analyzed. In the last part the results are summarized in a phase diagram.

### A. Effect of temperature on the magnetic field dependence of the polaron mass, the magnetization, and the susceptibility

From the preceding section it is apparent that with increasing temperature the effective electron-phonon interaction increases as long as the temperature does not exceed a specific value (see Fig. 13). Intuitively, one therefore expects that the critical point ( $\alpha = 4.2, \omega_c/\omega_0 = 2.24$ ) will shift to a smaller  $\alpha$  value and consequently also to a smaller magnetic field value (see Fig. 11) if the temperature increases. This will be confirmed by our numerical results.

In Fig. 15 the mass of the Feynman polaron perpendicular and parallel (see inset of figure) to the magnetic field is plotted as a function of the mag-

netic field for different values of the temperature. Note that the curves in Fig. 15 are quite similar to those in Fig. 7 [see also Figs. 9(a) and 9(b)] if  $\alpha$  is replaced by  $T$ . The Feynman polaron masses  $M_{\perp}=(v_{\perp}/w_{\perp})^2$  and  $M_{\parallel}=(v_{\parallel}/w_{\parallel})^2$  exhibit a discontinuity at a certain magnetic field value if the temperature is larger than 0.12.

The polaron magnetization ( $\mathcal{M}$ ) relative to the free-electron magnetization ( $\mathcal{M}_e$ ) is shown in Fig. 16(a) as a function of the magnetic field for different values of the temperature. A striking feature is that the electron-phonon contribution to the magnetization ( $\tilde{\mathcal{M}}=\mathcal{M}-\mathcal{M}_e$ ) is zero in the zero magnetic field limit. This is different from the zero-temperature case [see Fig. 3(a)] where  $\tilde{\mathcal{M}}$  is different from zero in the limit  $\omega_c/\omega_0 \rightarrow 0$ ; in other words,

$$\lim_{\omega_c \rightarrow 0} \lim_{T \rightarrow 0} \mathcal{M} \neq \lim_{T \rightarrow 0} \lim_{\omega_c \rightarrow 0} \mathcal{M}.$$

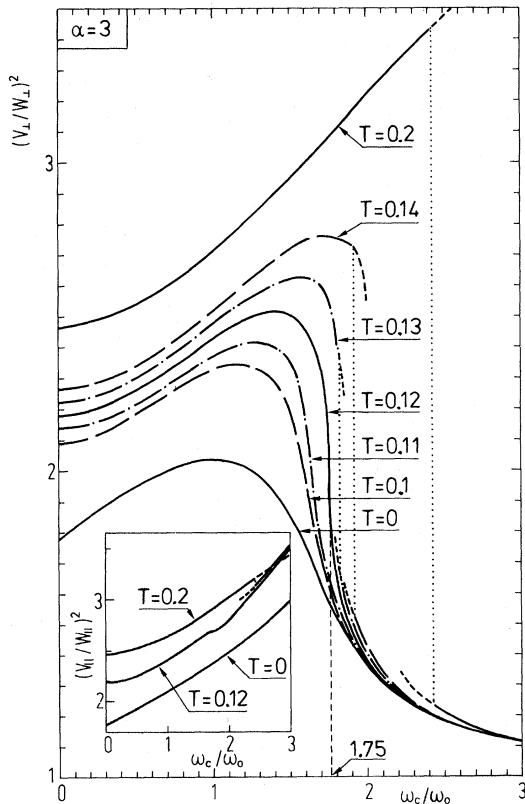


FIG. 15. Masses of the Feynman polaron perpendicular,  $M_{\perp}=(v_{\perp}/w_{\perp})^2$ , and parallel,  $M_{\parallel}=(v_{\parallel}/w_{\parallel})^2$ , to the magnetic field (inset of figure), as function of the magnetic field for different values of the temperature at a fixed electron-phonon coupling constant  $\alpha=3$ .

The analytic expression for the electron-phonon contribution to the magnetization for  $\alpha \ll 1$ ,  $\beta\omega_c \ll 1$ ,  $\beta \gg 1$  is [see Eq. (79) of paper I]

$$\tilde{\mathcal{M}} = \frac{\alpha}{36} \beta \omega_c \left[ 1 - \frac{3}{4\beta} + O\left(\frac{1}{\beta^2}\right) \right] + O(\alpha^2), \quad (12)$$

which indeed results in  $\tilde{\mathcal{M}}=0$  in the limit  $\omega_c \rightarrow 0$  if  $\beta$  is finite (thus  $T \neq 0$ ). Although expression (12) is only valid in the limit of weak coupling it is nevertheless suggestive for intermediate  $\alpha$ . Indeed, for small  $\omega_c/\omega_0$  values Eq. (12) results in a linear increase of  $\tilde{\mathcal{M}}$  as function of the magnetic field. The linear increase is steeper if the temperature is lower. As is apparent from Fig. 16(a) the same behavior is found numerically for  $\alpha=3$ .

The contribution of the electron-phonon interaction to the polaron susceptibility is shown in Fig. 16(b) around the critical point ( $T=0.120 \pm 0.001$ ,  $\omega_c/\omega_0=1.75 \pm 0.01$ ). In this point a second-order phase transition takes place. For temperatures<sup>34</sup> higher than  $0.12T_D$  the ideal polaron gas undergoes a first-order phase transition at a certain value of the magnetic field. For fixed  $\alpha$  (here  $\alpha=3$ ) one can draw,<sup>35</sup> in the  $(T/T_D, \omega_c/\omega_0)$  plane, a curve of first-order phase transitions that ends in a point where a second-order phase transition takes place (at the end of this section we will discuss this in more detail).

#### B. Effect of an external magnetic field on the temperature dependence of the polaron mass, the internal energy, the entropy, and the specific heat

In Fig. 17 the mass of the Feynman polaron perpendicular,  $M_{\perp}=(v_{\perp}/w_{\perp})^2$ , and parallel (see inset of figure),  $M_{\parallel}=(v_{\parallel}/w_{\parallel})^2$ , to the magnetic field is plotted as a function of the temperature for different values of the magnetic field. Observe that for low temperature there is a considerable difference between  $M_{\perp}$  and  $M_{\parallel}$ , which becomes even more pronounced as the temperature increases. However, above a well-defined temperature the difference between  $M_{\perp}$  and  $M_{\parallel}$  decreases if temperature increases further. For still higher temperatures the masses  $M_{\perp}$  and  $M_{\parallel}$  do not differ

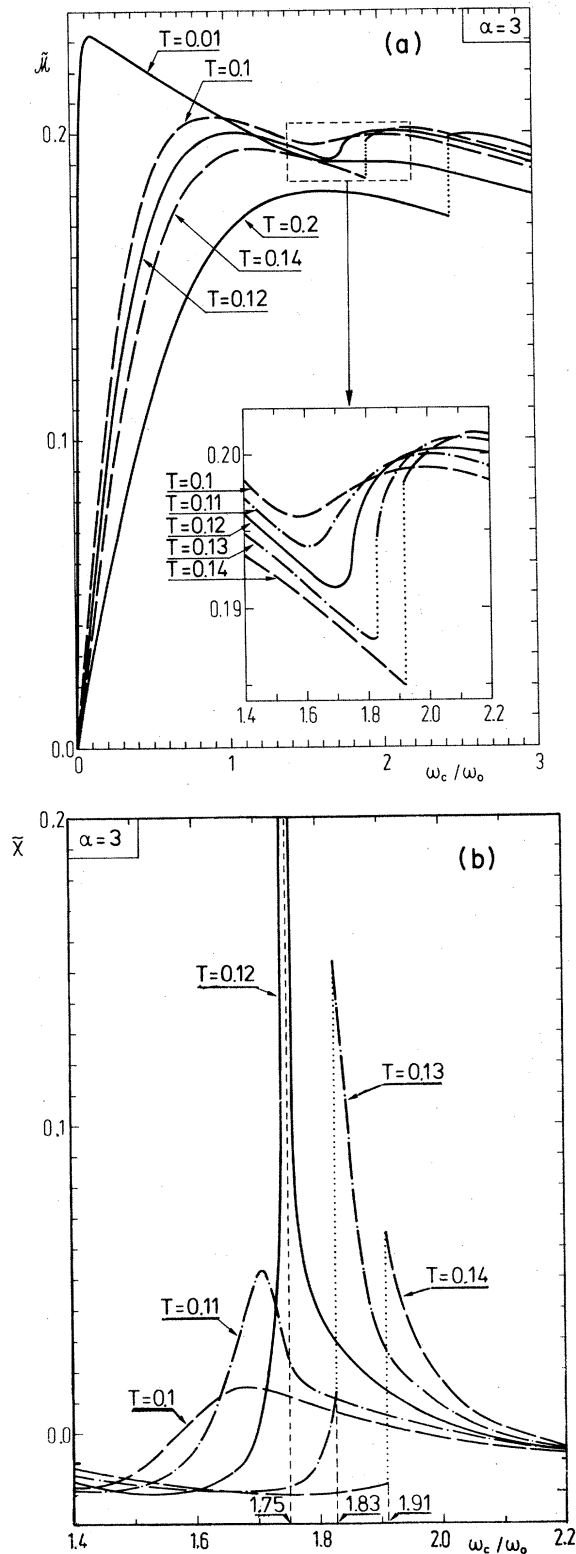


FIG. 16. Same as Fig. 15 but now for the contribution of the electron-phonon interaction to (a) magnetization (the inset represents an enlargement of the dashed rectangle) and (b) susceptibility.

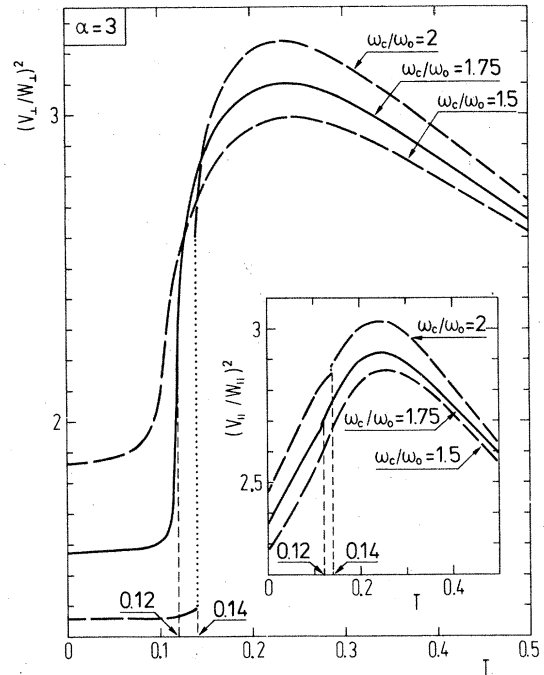


FIG. 17. Same as Fig. 15 but now as function of the temperature and at different values of the magnetic field.

very much, and furthermore, they are not very sensitive to changes of the magnetic field. This is due to the randomizing effect of temperatures which tends to restore the spherical symmetry in the effective electron-phonon interaction, leading to  $M_{\parallel} \approx M_{\perp}$ . Note that for  $\omega_c/\omega_0 > 1.75$  the Feynman polaron masses  $M_{\perp}$  and  $M_{\parallel}$  exhibit a discontinuity at a well-defined temperature.

The contribution of the electron-phonon interaction to the internal energy [Fig. 18(a)], the entropy [Fig. 18(b)], and the specific heat [Fig. 18(c)] are plotted as a function of the temperature for different values of the magnetic field. The application of an external magnetic field shifts the energy  $\tilde{E}$  curve to lower  $\tilde{E}$  values because the polaron self-energy increases with increasing magnetic field (see, e.g., Fig. 1 for the case  $\alpha = 1$ ). For the low temperature and low magnetic field behavior of the entropy  $\tilde{S}$  [see inset of Fig. 18(b)] we are in a situation that is quite similar to the one encountered earlier for the magnetization  $\tilde{M}$ , namely one has

$$\lim_{\omega_c \rightarrow 0} \lim_{T \rightarrow 0} \tilde{S} \neq \lim_{T \rightarrow 0} \lim_{\omega_c \rightarrow 0} \tilde{S}.$$

In the weak electron-phonon coupling limit this can be demonstrated analytically. From Eq. (67) of paper I we obtain for  $\alpha \ll 1$ ,  $\beta\omega_c \gg 1$ , and

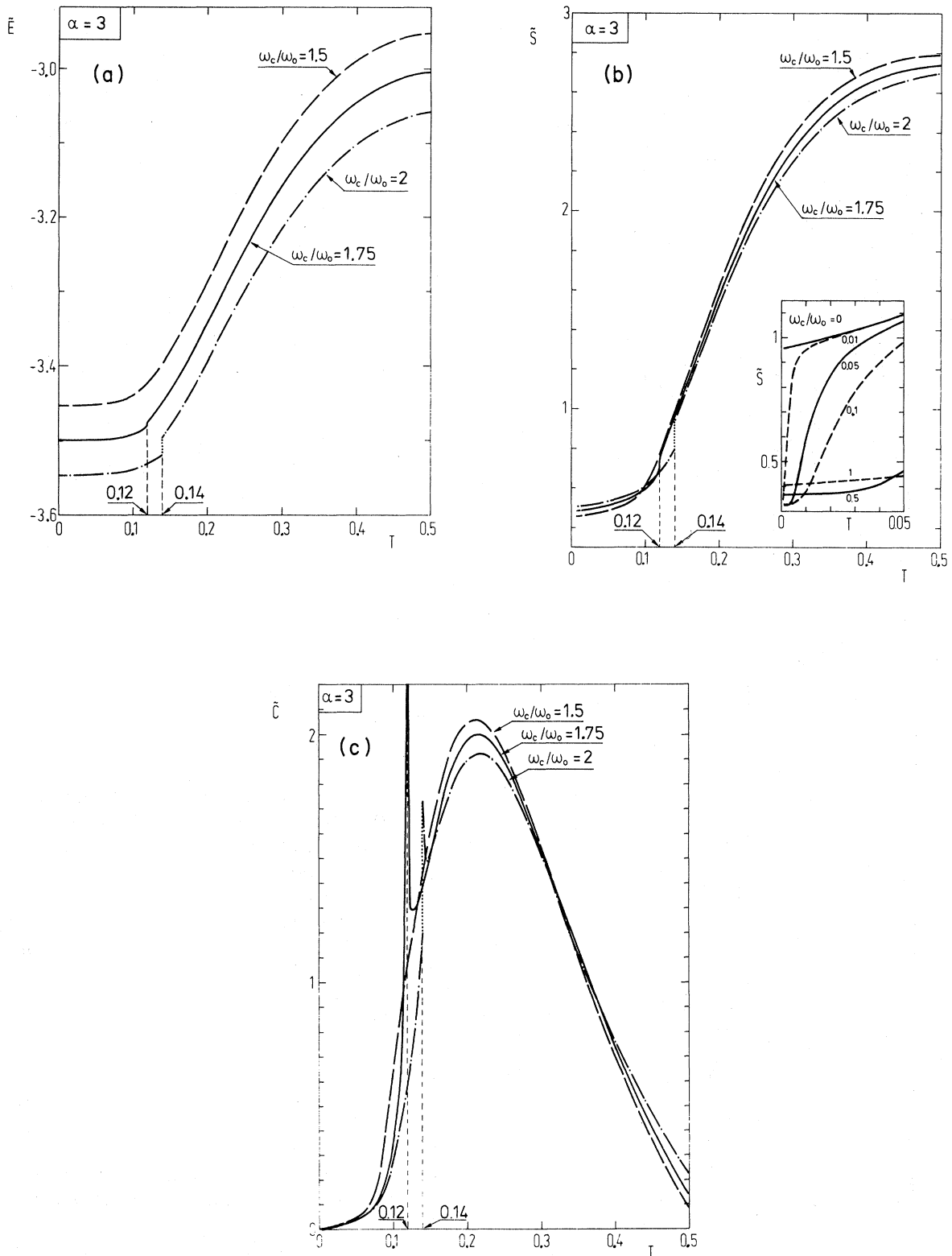


FIG. 18. Contribution of the electron-phonon interaction to (a) internal energy, (b) the entropy, and (c) specific heat. Plots are as a function of the temperature. Curves are drawn for different values of the magnetic field but at a fixed electron-phonon coupling constant, namely  $\alpha = 3$ .

$\omega_c \ll 1$  the following expression for the entropy per polaron:

$$\begin{aligned} \tilde{S} = & \frac{\alpha}{12} [1 + \frac{9}{20} \omega_c + O(\omega_c^2)] \\ & + \frac{81}{40} \frac{\alpha}{\beta} [1 - \frac{125}{48} \omega_c + O(\omega_c^2)] + O(\alpha^2), \end{aligned} \quad (13)$$

which gives

$$\lim_{\omega_c \rightarrow 0} \lim_{T \rightarrow 0} \tilde{S} = \frac{\alpha}{12} + O(\alpha^2),$$

while from Eq. (8) one obtains

$$\lim_{T \rightarrow 0} \lim_{\omega_c \rightarrow 0} \tilde{S} = \frac{\alpha}{4} + O(\alpha^2).$$

Furthermore, note that for very low temperature the entropy  $\tilde{S}$  increases with increasing magnetic field, while for higher values of the temperature the reverse is true [see Fig. 18(b)].

The specific heat  $\tilde{C}$  [Fig. 18(c)] diverges at the critical point<sup>34</sup>:  $(T/T_D, \omega_c/\omega_0) = (0.12, 1.75)$ . The

position of the broad peak in the  $\tilde{C}-T$  curve, which occurs at  $T/T_D = 0.20$  if  $\omega_c/\omega_0 = 0$  [see Fig. 14(c)], shifts slightly to higher temperature values if the magnetic field increases.

### C. Phase diagram

For  $T = 0$  the polaron state is determined by two physical parameters, namely the electron-phonon coupling constant  $\alpha$  and the magnetic field  $\mathcal{H}$  (or equivalently  $\omega_c/\omega_0$ ). The resulting phase diagram (see Fig. 11) is represented by a curve in the two-dimensional plane  $(1/\alpha, \omega_0/\omega_c)$ . In Fig. 19 we extended this phase diagram to arbitrary temperature. Now temperature is an additional physical parameter which is needed to characterize the phase of the polaron system. The points where a first-order phase transition takes place form a two-dimensional surface in the three-dimensional space  $(1/\alpha, \omega_0/\omega_c, T)$ . This surface intersects the

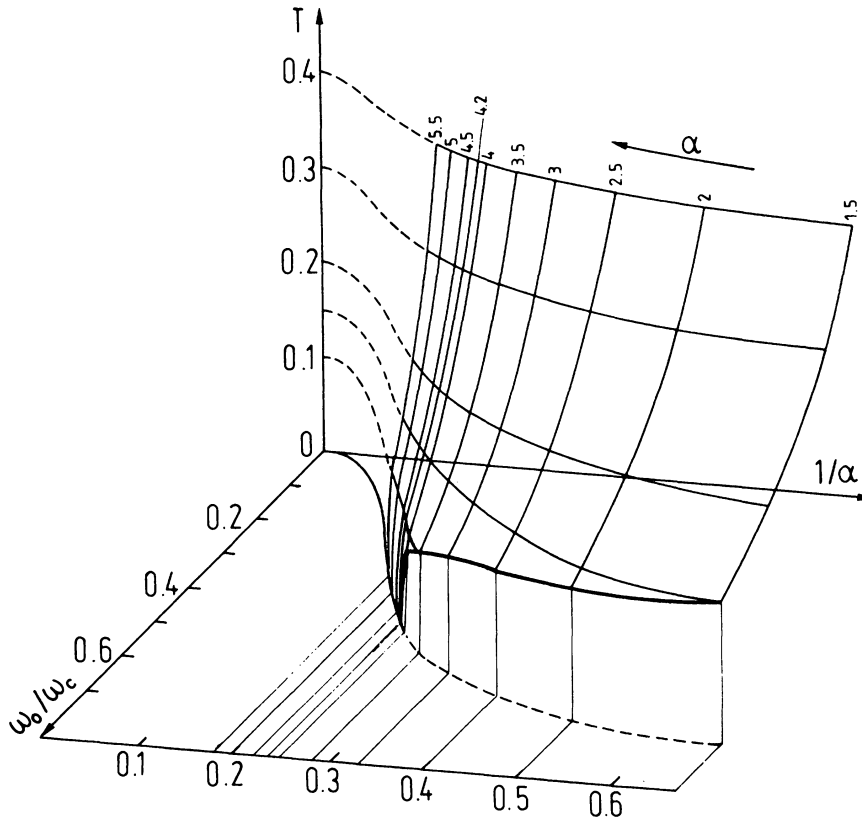


FIG. 19. Phase diagram. At the two-dimensional surface a first-order phase transition takes place. The solid, thick curve represents a critical line where a second-order phase transition takes place. At the front side of the surface, i.e., where  $\alpha \gg \omega_c/\omega_0$ , the polaron state is characterized by  $M_{\perp} \sim M_{\parallel}$ , while at the back side of the surface, i.e., where  $\alpha \ll \omega_c/\omega_0$ , one has  $M_{\parallel} \gg M_{\perp} \sim 1$ .

$T=0$  plane if  $\alpha \geq 4.2$ . The resulting curve is nothing more than the curve shown in Fig. 11. For  $\alpha < 4.2$  the surface does not intersect the  $T=0$  plane; it is confined by a line of second-order phase transitions (see, e.g., foregoing discussion on the numerical example  $\alpha=3$ ). In other words, the critical point ( $\alpha=4.2, \omega_0/\omega_c=2.24$ ) at  $T=0$  becomes a line of critical points, thus a *critical line* (thick and solid curve in Fig. 19), which circumscribes the surface of first-order phase transitions. This surface divides the physical space ( $1/\alpha, \omega_0/\omega_c, T$ ) into two regions in which the ideal polaron gas is in two different phases. In the region in front of the surface (where  $\omega_0/\omega_c \gg 1/\alpha$  or  $\alpha \gg \omega_c/\omega_0$ ) the polarons are characterized by  $M_\perp \sim M_\parallel$  (dressed state). On the other side of the surface (where  $\omega_0/\omega_c \ll 1/\alpha$  or  $\alpha \ll \omega_c/\omega_0$ ) the polarons are in the "stripped" state, i.e.,  $M_\parallel \gg M_\perp \sim 1$ .

The differences between the two polaron states can be summarized as follows.

- (1) The anisotropy in the effective electron-phonon interaction is small for polarons in the dressed state, i.e.,  $M_\parallel \sim M_\perp$ , while it is very large if the polarons are in the stripped state, i.e.,  $M_\parallel \gg M_\perp \sim 1$ .
- (2) The masses of the Feynman polaron,  $M_\perp$  and  $M_\parallel$ , are larger in the dressed polaron state than in the stripped polaron state.
- (3) The contribution of the electron-phonon interaction to the polaron magnetization  $\mathcal{M}$  is larger in the stripped state than in the dressed state.
- (4) In addition, the susceptibility  $\tilde{\chi}$  is larger in the stripped state than in the dressed state.
- (5) The internal energy  $\tilde{E}$  is lower for the stripped state than for the dressed state.
- (6) The entropy  $\tilde{S}$  is smaller if the polaron is stripped than if the polaron is dressed.
- (7) The contribution of the electron-phonon interaction to the specific heat  $\tilde{C}$  is larger for dressed polarons than for stripped polarons.

## VI. CONCLUDING REMARKS

In this section two topics are discussed. First, the difference between the present approach and a mean-field approach is outlined. This is of special importance in connection with the phase transition found in this work. In a second point the possible experimental consequences of our calculations are discussed briefly.

In mean-field theory the dynamical influence of the phonon field on the electron is replaced by the influence of an average field on the electron, or

equivalently, the electron moves in a *static* potential  $V(\vec{x})$ . In the path-integral formulation this mean-field theory leads to the following general form for the interacting part of the action (see also Sec. II of paper I):

$$S_{m,I} = \int_0^\beta du V(\vec{r}(u)). \quad (14)$$

This must be compared to the following form used in the present study (see Sec. III of paper I):

$$S_{m,I} = \int_0^\beta du \int_0^\beta ds W(\vec{r}(u) - \vec{r}(s); u - s), \quad (15)$$

where  $W(\vec{r}; \tau)$  is a certain function quadratic in  $\vec{r}$  that depends on four parameters  $v_\perp, v_\parallel, w_\perp, w_\parallel$ . This action, given by Eq. (15), can be considered as containing a *dynamical* potential that not only depends on the position of the electron at a given moment but also depends on the whole electron path between the (imaginary) times 0 and  $\beta$ . Thus in Eq. (15) a *memory* effect is taken into account. Therefore, the present approach goes beyond mean-field theory. Note that if we take  $w_\perp = w_\parallel = 0$  in Eq. (15) [see also Eq. (28) of Sec. III of paper I] the double-time integral in Eq. (15) can be reduced to a single one, and thus Eq. (15) reduces to the form of Eq. (14). Thus the mean-field theoretical approach is contained in our theory as a special case.

Now we will discuss the possible experimental consequences of the results reported here. These consequences are twofold, namely, the phase transition will have implications on the static polaron quantities, i.e., the thermodynamic quantities, and on the dynamic polaron quantities, for example, the magneto-optical absorption. Let us first discuss the effect on the thermodynamic quantities like the specific heat and the susceptibility. Intuitively, one expects that due to the relatively small number of conduction electrons (and thus of polarons) in ionic crystals and polar semiconductors the contribution of the electron-phonon interaction (and also of the electrons themselves) will be negligible in comparison with the contribution of the ions. To check the validity of this assertion let us take four typical polar semiconductors KCl, KBr, AgCl, and AgBr, which have, respectively, the following values for the electron-phonon coupling constant<sup>36,37</sup>:  $\alpha = 3.44, 3.05, 1.94,$  and  $1.56$ . These four crystals have a face-centered-cubic structure. It has been shown<sup>38,39</sup> that for such dielectric crystals the specific heat (expressed in  $\text{cal K}^{-1} \text{mol}^{-1}$ ) is given by

$$C_V = 928.6 \left[ \frac{T}{\Theta} \right]^3 \quad (16)$$

if the temperature<sup>40</sup>  $T < \Theta/50$  ( $\Theta$  is called the Debye temperature and  $C_V$  is the specific heat at constant volume. The specific heat discussed in the foregoing sections is also taken at constant volume). In general, for  $T < \Theta/50$  the specific heat no longer follows a simple  $T^3$  behavior because positive terms are added<sup>40</sup> to Eq. (16). To obtain a lower bound to the crystal specific heat we may use Eq. (16) also for  $T < \Theta/50$ . Note that the Debye temperature and the temperature<sup>34</sup>  $T_D$ , which was used as unit temperature here, differ slightly. For the above materials KCl, KBr, AgCl, and AgBr one has, respectively,<sup>36,37,41</sup>  $\Theta (T_D) = 235$  (305), 174 (240), 183 (260), and 144 (190). As an example take  $T/T_D = 0.01, 0.1, \text{ and } 0.2$ ; it then follows that the specific heat of the above four materials is, respectively, of the order  $10^{-5} - 10^{-4}, 10^{-2} - 10^{-1}, \text{ and } 0.4 - 0.9 \text{ cal K}^{-1} \text{ cm}^{-3}$ . The contribution of the electron-phonon interaction to the specific heat (for  $\alpha \sim 3.5$ ) is about  $C \sim 0.01$  for  $T/T_D = 0.01, 1.0$  for  $T/T_D = 0.1, \text{ and } 2.5$  for  $T/T_D = 0.2$  [see, e.g., Figs. 14(c) and 18(c)] as expressed in dimensionless units. The density of conduction electrons (and thus polarons) in those materials is typically of the order<sup>42</sup>  $10^6 - 10^7 \text{ cm}^{-3}$ , for the considered temperature range. For these polaron densities the contribution of the electron-phonon interaction to the specific heat (in units  $\text{cal K}^{-1} \text{ cm}^{-3}$ ) is of the order  $3 \times 10^{20} - 3 \times 10^{-19}$  for  $T/T_D = 0.01, 3 \times 10^{-18} - 3 \times 10^{-17}$  for  $T/T_D = 0.01, \text{ and } 8 \times 10^{-18} - 8 \times 10^{-17}$  for  $T/T_D = 0.2$ . These values are at least 15 orders of magnitude smaller than the values for the total specific heat. Even if the electron density is as high as  $10^{13} \text{ cm}^{-3}$  the polaron contribution is still 8 orders of magnitude smaller than the total specific heat, and thus negligible.

For the magnetic susceptibility the same can be shown. The diamagnetic susceptibility of<sup>43</sup> KCl, KBr, AgCl, and AgBr is  $-39.0 \times 10^{-6}, -49.1 \times 10^{-6}, -49.0 \times 10^{-6}, \text{ and } -59.7 \times 10^{-6}$  (as expressed in cgs units). The contribution of the electron-phonon interaction to the susceptibility (using the same units as before) is of order  $10^{-19}$  if  $n_e = 10^6 \text{ cm}^{-3}$  and of order  $10^{-12}$  if  $n_e = 10^{13} \text{ cm}^{-3}$  ( $n_e$  is the electron density) and thus again negligible in comparison to the total susceptibility of those polar materials. As a consequence it would be very difficult, if not impossible, to detect experimentally the first-order phase transition via the thermodynamic quantities. Degenerate polar semiconductors have a much higher electron density ( $n_e \sim 10^{16} - 10^{20}$ ). However, those materials are

weakly polar (e.g., GaAs has  $\alpha = 0.068$ ). The polaron contribution to the specific heat of such materials is at most a few tenth of a percent while for the magnetic susceptibility it is at most a few percent.

The parameters of the Feynman polaron  $v_{\perp}, v_{\parallel}, w_{\perp}, w_{\parallel}$  exhibit a discontinuity at the phase-transition point. This discontinuity will reflect itself in a discontinuous behavior of the magneto-optical absorption spectrum as a function of the magnetic field. In particular, we expect that the cyclotron-resonance line will show a sudden shift at the transition point. The calculation of this shift is nontrivial. At present we limit ourselves to present values of the temperature and the magnetic field at which the second-order phase transition occurs, for several semiconductors. These values are presented in Fig. 20. To observe the first-order polaron phase transition one should apply magnetic fields slightly larger (see Fig. 19) than the values indicated in Fig. 20. The effect of the transition will be larger if the jump in  $M_{\perp}$  at the transition point (indicated by  $\Delta M_{\perp}$ ) is larger. In Fig. 21 a plot is made of  $\Delta M_{\perp}$  as a function of temperature for  $\alpha = 3$ . For  $T/T_D < 0.12$  there is no phase transition and thus  $\Delta M_{\perp} = 0$ . The largest discontinuity in  $M_{\perp}$  occurs around  $T/T_D = 0.4$  where  $\Delta M_{\perp} = 2.76$ . With increasing magnetic field the mass  $M_{\perp}$  decreases suddenly from  $3.87m$  to  $1.11m$

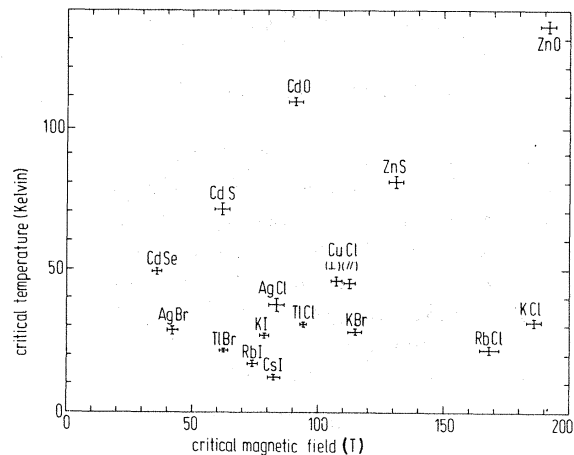


FIG. 20. Value of the critical temperature and critical magnetic field for sixteen compound semiconductors. For CuCl the values of the transverse ( $\perp$ ) and longitudinal ( $\parallel$ ) electron are shown. The error bars originate from (1) the spreading in the values for  $\alpha, \omega_0,$  and  $m$  as reported in the literature (Refs. 36 and 37) and (2) from the numerical inaccuracy in the determination of the critical point.

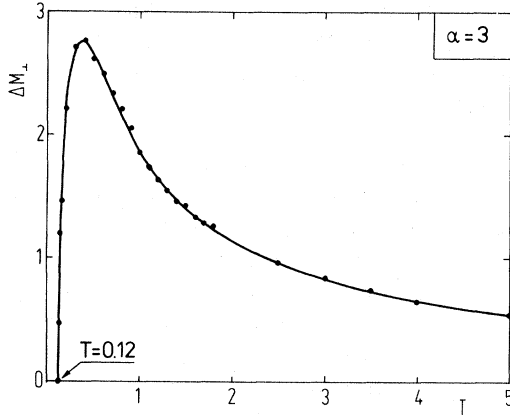


FIG. 21. Temperature dependence of the jump in the mass  $M_1$  at the phase transition point for  $\alpha=3$ .

( $m$  is the electron band mass), which is a decrease with a factor of 3.5.

The magnetic field range indicated in Fig. 20 is experimentally accessible by the use of pulsed magnetic fields.<sup>44</sup> These magnetic fields have a pulse duration of the order of microseconds. The polaron needs only a time of the order of a few picoseconds to relax to equilibrium; this time interval is 6 orders of magnitude smaller than the pulse duration of the magnetic field. As a consequence it is possibly worthwhile to perform a magneto-optical experiment (see, e.g., Refs. 44 and 45) to investigate the phase transition of an ideal polaron gas found in the present theoretical work.

#### ACKNOWLEDGMENTS

The authors are grateful to Professor R. Elliott, Dr. S. Komiyama, Professor F. Mueller, and Professor W. Richter for interesting discussions. Financial support by Fonds voor Kollektief Onderzoek, Belgium; Project No. 2.0072.80 (FKFO) is gratefully acknowledged. One of us (F.P.) is grateful to the National Fund for Scientific Research (Belgium) for financial support.

#### APPENDIX A

In this appendix we calculate the polarization charge density induced by the electron; in other words we will calculate the density of the polarization cloud of the polaron. The interaction term in the Fröhlich Hamiltonian is proportional to the electrostatic potential operator (see Ref. 46)

$$\Phi(\vec{r}) = -\frac{1}{e} \sum_{\vec{k}} (V_{\vec{k}} a_{\vec{k}} e^{i\vec{k}\cdot\vec{r}} + V_{\vec{k}}^* a_{\vec{k}}^\dagger e^{-i\vec{k}\cdot\vec{r}}), \quad (\text{A1})$$

which leads to a polarization charge-density operator

$$\rho(\vec{r}) = -\frac{1}{4\pi} \nabla^2 \Phi(\vec{r}). \quad (\text{A2})$$

After taking the ensemble average of Eq. (A2) one obtains the polarization charge density surrounding the electron,

$$\begin{aligned} \rho(\vec{r}) &= \langle \rho(\vec{r} - \vec{x}) \rangle \\ &= -\frac{1}{4\pi e} \sum_{\vec{k}} k^2 (V_{\vec{k}} e^{-i\vec{k}\cdot\vec{r}} \langle a_{\vec{k}} e^{i\vec{k}\cdot\vec{x}} \rangle \\ &\quad + V_{\vec{k}}^* e^{i\vec{k}\cdot\vec{r}} \langle a_{\vec{k}}^\dagger e^{-i\vec{k}\cdot\vec{x}} \rangle), \end{aligned} \quad (\text{A3})$$

where  $\vec{x}$  is the electron position operator. If the interaction coefficients  $V_{\vec{k}}$  and  $V_{\vec{k}}^*$  in the Fröhlich Hamiltonian [see Eqs. (1)–(4) of paper I] are considered as independent variables one obtains for the expectation values in Eq. (A3)

$$B_{\vec{k}} = \langle a_{\vec{k}} e^{i\vec{k}\cdot\vec{x}} \rangle = -\frac{1}{\beta} \frac{1}{Z} \frac{\partial Z}{\partial V_{\vec{k}}}, \quad (\text{A4})$$

$$B_{\vec{k}}^* = \langle a_{\vec{k}}^\dagger e^{-i\vec{k}\cdot\vec{x}} \rangle = -\frac{1}{\beta} \frac{1}{Z} \frac{\partial Z}{\partial V_{\vec{k}}^*}, \quad (\text{A5})$$

with  $Z$  the partition function. In the path-integral representation Eq. (A4) becomes [see Eqs. (6) and (8c) of paper I]

$$B_{\vec{k}} = -\frac{1}{\beta} \left\langle \frac{\partial S[\vec{x}]}{\partial V_{\vec{k}}} \right\rangle, \quad (\text{A6})$$

where the average  $\langle \rangle$  is defined in terms of path integrals. Equation (A6) will be evaluated approximately. As in paper I, the average  $\langle \rangle$  over the exact ensemble is replaced by an average  $\langle \rangle_m$  over the ensemble corresponding with the anisotropic Feynman polaron model [see Eqs. (10) and (15) of paper I]. For the evaluation of the approximation average we refer to Secs. II and III of paper I, where all the essential steps can be found. Equation (A6) becomes equal to

$$B_{\vec{k}} = -V_{\vec{k}}^* (1 + n(\omega_0)) \int_0^\beta du e^{-u} e^{-k^2 D(u)} e^{-k^2 D_H(u)}, \quad (\text{A7})$$

where the same notations have been used as in pa-

per I [the function  $D(u)$  and  $D_H(u)$  are given, respectively, by Eqs. (49a) and (49b) of paper I]. Inserting Eq. (A7) [and using Eq. (A5)] into Eq. (A3) one obtains

$$\rho(\vec{r}) = \frac{\sqrt{2}\alpha}{(2\pi)^3 e} [1 + n(\omega_0)] \times \int d\vec{k} e^{-i\vec{k}\cdot\vec{r}} \times \int_0^\beta du e^{-u} e^{-k_z^2 D(u)} e^{-k_\perp^2 D_H(u)}, \quad (\text{A8})$$

and after performing the  $\vec{k}$  integral one finds

$$\rho(\vec{r}) = \frac{\alpha}{2^{5/2} \pi^{3/2} e} [1 + n(\omega_0)] \times \int_0^\beta du \frac{e^{-u}}{\sqrt{D(u)D_H(u)}} \times \exp\left[-\frac{x^2 + y^2}{4D_H(u)^2} - \frac{z^2}{4D(u)^2}\right]. \quad (\text{A9})$$

In the limit of zero temperature ( $T=0$ ), small electron-phonon coupling ( $\alpha \ll 1$ ), and zero magnetic field ( $\omega_c/\omega_0=0$ ), one has  $D(u)=D_H(u)=u/2$ , and Eq. (A9) reduces to

$$\rho(\vec{r}) = \frac{\alpha}{\pi\sqrt{2}e} \frac{\exp(-\sqrt{2}|\vec{r}|)}{|\vec{r}|}, \quad (\text{A10})$$

which is the result already obtained in Ref. 46.

Another limiting case for which  $\rho(\vec{r})$  can be evaluated exactly is the one in which  $T=0$ ,  $\alpha \ll 1$ , and  $\omega_c/\omega_0 \gg 1$  (large magnetic fields). In this case we have  $D(u)=u/2$  and

$$D_H(u) = (1 - e^{-\omega_c u})/2\omega_c \sim 1/2\omega_c.$$

Inserting these expressions into Eq. (A8) and evaluating the integrals, one obtains for  $\vec{r} \neq 0$ ,

$$\rho(\vec{r}) = \frac{\alpha}{2\pi e} \omega_c \exp\left[-(x^2 + y^2)\frac{\omega_c}{2} - \sqrt{2}z\right]. \quad (\text{A11})$$

Thus for  $T=0$  and  $\alpha \ll 1$  we found [see Eq. (A10)] that in the absence of a magnetic field the induced polarization is spherical symmetric; the polaron radius is of the order of  $1/\sqrt{2}$ . For large magnetic fields the polaron is strongly anisotropic. Along the magnetic field [take, for example,  $x=y=0$  in Eq. (A11)] the polarization increases with increasing magnetic field strength. This will result in an enhancement of the polaron mass,  $M_{\parallel}$ , along the magnetic field. Perpendicular to the magnetic field [for example, take  $z=0$  in Eq. (A11)] the polaron radius is of the order  $\sqrt{2}/\omega_c$ , which decreases with increasing magnetic field. And consequently the polaron mass,  $M_{\perp}$ , perpendicular to the magnetic field, will decrease to the bare-electron band mass in the limit  $\omega_c/\omega_0 \rightarrow \infty$ .

<sup>1</sup>F. M. Peeters and J. T. Devreese, preceding paper, Phys. Rev. B **26**, 7281 (1982).

<sup>2</sup>R. P. Feynman, Phys. Rev. **27**, 660 (1955).

<sup>3</sup>R. W. Hellwarth and P. M. Platzman, Phys. Rev. **128**, 1599 (1962).

<sup>4</sup>M. Saitoh, J. Phys. Soc. Jpn. **49**, 886 (1980); K. Arisawa and M. Saitoh, Phys. Lett. **82A**, 462 (1980).

<sup>5</sup>M. Saitoh, J. Phys. Soc. Jpn. **50**, 2295 (1981).

<sup>6</sup>F. M. Peeters and J. T. Devreese, Solid State Commun. **39**, 445 (1981).

<sup>7</sup>E. P. Gross, Ann. Phys. **8**, 78 (1959).

<sup>8</sup>D. M. Larsen, in *Polarons in Ionic Crystals and Polar Semiconductors*, edited by J. T. Devreese (North-Holland, Amsterdam, 1972), p. 237.

<sup>9</sup>D. Matz and B. C. Burkey, Phys. Rev. B **3**, 3487 (1971).

<sup>10</sup>J. M. Luttinger and C. Y. Lu, Phys. Rev. B **21**, 4251 (1980).

<sup>11</sup>R. Manka, Phys. Lett. **67A**, 311 (1978); Phys. Status Solidi B **93**, 53 (1979); R. Manka and M. Suffczynski, J. Phys. C **13**, 6369 (1980).

<sup>12</sup>Y. Lépine and D. Matz, Phys. Status Solidi B **96**, 797 (1979).

<sup>13</sup>As far as Ref. 8 is concerned we refer only to the last part of Ref. 8 where the bound polaron is discussed. There Larsen found a discontinuous shrinking of the polaron wave function as function of  $\alpha$ . This transition found by Larsen is closely related to the localization type of transition found by some authors (Refs. 7 and 9–12).

<sup>14</sup>F. M. Peeters and J. T. Devreese, Phys. Status Solidi B (in press).

<sup>15</sup>Y. Toyozawa, Progr. Theor. Phys. **26**, 29 (1961); in *Polarons and Excitons*, edited by C. G. Kuper and G. D. Whitfield (Oliver and Boyd, Edinburgh, 1963), p. 211; A. Sumi and Y. Toyozawa, J. Phys. Soc. Jpn. **35**, 137 (1973).

<sup>16</sup>D. M. Larsen, Phys. Rev. **180**, 919 (1969).

<sup>17</sup>The radius of the electron wave function, parallel or perpendicular to the magnetic field, will always be referred to the center-of-mass system of the polaron.

<sup>18</sup>To obtain the magnetization and the susceptibility in

dimensional units one must multiply the magnetization by  $e\hbar/mc$  and the susceptibility by  $e^2\hbar/m^2c^2\omega_0$ .

- <sup>19</sup>L. D. Landau, *Z. Phys.* **64**, 629 (1930).
- <sup>20</sup>This procedure is outlined in the article by C. H. Reinsch, *Numer. Math.* **10**, 177 (1967). We are indebted to Dr. F. Brosens for providing us the numerical program.
- <sup>21</sup>M. Abramowitz and I. A. Stegun, *Handbook of Mathematical Functions* (Dover, New York, 1968), p. 877.
- <sup>22</sup>Y. Lépine and D. Matz, *Can. J. Phys.* **54**, 1979 (1976).
- <sup>23</sup>R. Evrard, E. Kartheuser, and J. Devreese, *Phys. Status Solidi B* **41**, 431 (1970), hereafter referred to as EKD.
- <sup>24</sup>E. P. Kartheuser and P. Negrete, *Phys. Status Solidi B* **57**, 77 (1973), hereafter referred to as KN.
- <sup>25</sup>D. M. Larsen, *Phys. Rev.* **172**, 967 (1968).
- <sup>26</sup>J. Adamowski, B. Gerlach and H. Leschke, in *Functional Integration: Theory and Application*, edited by J. P. Antoine and E. Tirapequi (Plenum, New York, 1980), p. 291.
- <sup>27</sup>J. T. Marshall and M. S. Chawla, *Phys. Rev. B* **10**, 4283 (1970).
- <sup>28</sup>K. Huang, *Statistical Mechanics*, (Wiley, New York, 1963).
- <sup>29</sup>F. M. Peeters and J. T. Devreese, *Phys. Status Solidi B* (in press); in *Recent Developments in Condensed Matter Physics*, Proceedings of the 1980 Conference of the Condensed Matter Division of the EPS, edited by J. T. Devreese, L. F. Lemmens, V. E. Van Doren, and J. Van Royen (Plenum, New York, 1981), Vol. 3, p. 373.
- <sup>30</sup>G. R. Allcock, *Adv. Phys.* **5**, 412 (1956).
- <sup>31</sup>R. Kubo, *Statistical Mechanics* (North-Holland, Amsterdam, 1971).
- <sup>32</sup>L. D. Landau and E. M. Lifshitz, *Statistical Physics*, (Pergamon, New York, 1970), p. 263.
- <sup>33</sup>Y. Osaka, *J. Phys. Soc. Jpn.* **21**, 423 (1966).
- <sup>34</sup>The unit of temperature is  $T_D = \hbar\omega_0/k_B$ .  $k_B$  is the Boltzmann constant. The units of entropy and specific heat are both equal to  $k_B$ .
- <sup>35</sup>F. M. Peeters and J. T. Devreese, *Solid State Commun.* **41**, 49 (1982).
- <sup>36</sup>E. Kartheuser, in *Polarons in Ionic Crystals and Polar Semiconductors*, Ref. 8, p. 717.
- <sup>37</sup>J. T. Devreese, J. Van Royen, and M. Mariën (unpublished).
- <sup>38</sup>P. Debye, *Ann. Phys.* **39**, 789 (1912).
- <sup>39</sup>M. Born and T. von Karman, *Z. Phys.* **13**, 297 (1912).
- <sup>40</sup>W. W. Scales, *Phys. Rev.* **112**, 49 (1958).
- <sup>41</sup>E. W. Kaye and T. H. Laby, *Tables of Physical and Chemical Constants* (Longman, London, 1973), p. 55.
- <sup>42</sup>See, e.g., S. Komiyama, T. Masumi, and K. Kajita, *Phys. Rev. B* **20**, 5192 (1979).
- <sup>43</sup>R. C. Weast, *Handbook of Chemistry and Physics*, 53rd ed. (Chemical Rubber Co., Ohio, 1972), p. E-109.
- <sup>44</sup>See, e.g., E. Kido, N. Miura, E. Kawauchi, I. Ogura, J. F. Dillon, Jr., and S. Chikazumi, *Physica* **89B**, 147 (1977).
- <sup>45</sup>N. Miura, G. Kido, and S. Chikazumi, *Solid State Commun.* **18**, 885 (1976).
- <sup>46</sup>T. D. Lee, F. E. Low, and D. Pines, *Phys. Rev.* **90**, 297 (1953).